

**THE UNIVERSITY OF WESTERN ONTARIO
DEPARTMENT OF CIVIL AND
ENVIRONMENTAL ENGINEERING**

Water Resources Research Report

**The Comparison of GEV, Log-Pearson Type 3
and Gumbel Distributions in the
Upper Thames River Watershed
under Global Climate Models**

**By:
Nick Millington
Samiran Das
and
S. P. Simonovic**

**Report No: 077
Date: September 2011**

**ISSN: (print) 1913-3200; (online) 1913-3219;
ISBN: (print) XXX-X-XXXX-XXXX-X; (online) XXX-X-XXXX-XXXX-X;**



**The Comparison of GEV, Log-Pearson Type 3 and Gumbel
Distributions in the Upper Thames River Watershed under
Global Climate Models**

By

Nick Millington
Samiran Das
and
Slobodan P. Simonovic

Department of Civil and Environmental Engineering
The University of Western Ontario
London, Ontario, Canada

September 2011

Table of Contents

LIST OF TABLES	3
LIST OF FIGURES	4
EXECUTIVE SUMMARY	5
1. INTRODUCTION	6
1.1 CLIMATE CHANGE AND WATER RESOURCE MANAGEMENT	6
1.2 STATISTICAL ANALYSIS OF CLIMATE CHANGE DATA	7
1.3 STATISTICAL TOOLS.....	7
1.4 OBJECTIVE OF THE STUDY	8
1.5 RESEARCH PROCEDURE	8
1.6 ORGANIZATION OF THE REPORT	9
2. METHODOLOGY	10
2.1 STATISTICAL DISTRIBUTIONS	10
2.1.1 <i>Generalized Extreme Value Distribution (GEV)</i>	10
2.1.2 <i>Gumbel Distribution (EV1)</i>	11
2.1.3 <i>Log Pearson Type 3 Distribution (LP3)</i>	12
2.2 PARAMETER ESTIMATION TECHNIQUES.....	13
2.2.1 <i>Probability Weighted Moments Equations</i>	13
2.2.2 <i>L-Moment Equations</i>	14
2.2.3 <i>Generalized Extreme Value</i>	15
2.2.4 <i>Gumbel (EV1)</i>	16
2.2.5 <i>Log Pearson Type 3</i>	17
2.3 GOODNESS OF FIT TESTS.....	17
2.3.1 <i>Anderson-Darling Test</i>	18
2.3.2 <i>Kolmogorov-Smirnov Test</i>	18
2.3.3 <i>Chi-Squared Test</i>	19
2.3.4 <i>L-Moment Ratio Diagrams</i>	19
2.4 INTENSITY DURATION FREQUENCY CURVES & STORM DURATIONS.....	20
2.4.1 <i>Storm Durations</i>	21
3. CASE STUDY	23
3.1 STUDY AREA: THE UPPER THAMES RIVER WATERSHED.....	23
3.2 INPUT DATA	23
3.2.1 <i>Historical Data</i>	23
3.2.2 <i>Data Manipulation</i>	24
3.2.3 <i>Description of AOGCM Models</i>	25
3.2.4 <i>Emission Scenarios</i>	26
3.3 RESULTS.....	27
3.3.1 <i>Goodness of Fit Tests</i>	27
3.3.2 <i>L-Moment Ratio Diagrams</i>	28
3.3.3 <i>Shape Parameter</i>	29
3.4 GEV RETURN VALUES & UNCERTAINTIES	32
3.4.1 <i>Return Values</i>	35
3.4.2 <i>IDF Curves</i>	37
4. CONCLUSIONS	39
REFERENCES	41

APPENDIX A: FIGURES	43
APPENDIX B: PREVIOUS REPORTS IN THE SERIES.....	47

List of Tables

Table 3.1: Summary of AOGCMs and emission scenarios

Table 3.2: Number of rejections at the 5% significance level for the 3 goodness of fit tests

Table 3.3: Shape Parameter values for all AOGCM data sets

Table 3.4: Summary of quartile information for shape parameter boxplot

Table 3.5(a): Depth of precipitation (mm) for ECHAM5AOM_A1B

Table 3.5(b): Depth of precipitation (mm) for MIROC3MEDRES_A2

Table 3.5(c): Depth of precipitation (mm) for Environment Canada

Table 3.6(a): Percent Difference between ECHAM5AOM_A1B and EC

Table 3.6(b): Percent Difference between MIROC3MEDRES_A2 and EC

Table 3.7(a): Percent Difference between ECHAM5AOM_A1B and Historical Perturbed

Table 3.7(b): Percent Difference between MIROC3MEDRES_A2 and Historical Perturbed

List of Figures

Figure 3.1: L-Moment Ratio Diagram for 12-hour storm duration

Figure 3.2: Boxplot of shape parameter values for all 5 storm durations

Figure 3.3(a): 1-Hour Duration Return Values

Figure 3.3(b): 2-Hour Duration Return Values

Figure 3.3(c): 6-Hour Duration Return Values

Figure 3.3(d): 12-Hour Duration Return Values

Figure 3.3(e): 24-Hour Duration Return Values

Figure 3.4(a): 2-Year IDF Curve

Figure 3.4(b): 5-Year IDF Curve

Figure 3.4(c): 10-Year IDF Curve

Figure 3.4(d): 25-Year IDF Curve

Figure 3.4(e): 50-Year IDF Curve

Figure 3.4(f): 100-Year IDF Curve

Executive Summary

The increase in greenhouse gas emissions has had a severe impact on global temperature, and is affecting weather patterns worldwide. With this global climate change, precipitation levels are changing, and in many places are drastically increasing. The need to be able to accurately predict extreme precipitation events is imperative in designing for not only the safety of infrastructure, but also people's lives. To predict these events, the use of historical data is necessary, along with statistical distributions that are used to fit the data.

In this study, historical data from the London International Airport station has been used, along with 11 different Atmosphere Ocean Global Climate Models (AOGCMs), which are used to predict future climate variables. These models produced a total of 27 different data sets of annual maximum precipitation over a period of 117 years, for storm durations of 1, 2, 6, 12 and 24 hours.

The current Environment Canada recommended distribution is the Gumbel (EV1) distribution, and the current United States distribution is the Log-Pearson type 3 (LP3). This report investigates a third distribution, the Generalized Extreme Value (GEV) distribution, in the context of the Upper Thames River Watershed.

The historical data set and the data sets derived from AOGCMs were used with the GEV, LP3 and EV1 distributions, and the goodness of fit tests were performed to select which was most appropriate distribution. L-Moment Ratio diagrams were also constructed to help establish the most suitable distribution. All results showed that GEV was very appropriate to the Upper Thames River Watershed data, and it was often the favored distribution.

This report shows the need for more studies to be carried out on the GEV distribution, to ensure we are using the most appropriate methods for predicting these extreme precipitation events.

1. Introduction

1.1 Climate Change and Water Resource Management

The increased use of fossil fuels across the globe has led to a substantial rise in greenhouse gas emissions worldwide. The scientific community has directly linked these CO₂ emissions to climate change. The rising temperature will have many effects on the environment, and on hydrological processes. These effects will undoubtedly influence the frequency and severity of floods and droughts experienced in many areas of the world. Addressing and understanding these effects on the climate is essential to ensure that the population is prepared to cope with the changes. Predicting the effects that the rising temperature will have on precipitation patterns is necessary to safely plan for the future. Severe weather can have a tremendous affect on the environment, local infrastructure, and the general population.

In order to accurately design and manage flood control structures, including sewers, reservoirs and dams, an appropriate way of estimating these extreme events must be determined. Engineers, as well as many other professions, have the responsibility of accurately assessing these risks and taking them into account during the design process. In a 2007 report from the Inter-governmental Panel on Climate Change (IPCC, 2007), it is predicted that precipitation intensities will increase world wide, particularly in mid to high latitudes. Studying these changing patterns is crucial in being able to estimate future extreme climatic events, such as temperature and precipitation intensity. Looking at the extremes is vitally important as these values could present much greater risk to the population, compared with the mean increases alone. The change in climate will in turn increase the risk of flash flooding and urban flooding, and has the potential to incur a vast amount of monetary damage and endanger human lives. The capacity of current city infrastructure, including storm drain systems, may need to be evaluated to check if they are adequately prepared to handle the increased risk of flooding. The intensities and frequency of these rains and floods will vary over the globe, however already in some locations the current 100-year design flood is estimated to occur every 2 to 5 years. (IPCC, 2007)

1.2 Statistical Analysis of Climate Change Data

The use of statistics has a wide range of important applications in climate research, as climatology can be said to be the study of the statistics of our climate (Storch, 1999). These applications can range from simple calculations of the means, and measures of variability of the data, which is used to predict future events, but also include, advanced methods that investigate the dynamics of the climate system. The use of statistical distributions is applied to historical data, which is fit to the desired distribution. The parameters of the distribution are estimated, and from this information, the Cumulative Density Function (CDF) and Probability Density Function (PDF) are created. The distributions are also used to estimate the probability of future maximum occurrences, which is needed for design and planning. Historical climate data in Canada is available to the public from Environment Canada website. This data includes daily and monthly temperature and precipitation data, dating back to various years depending on the station in question.

As the climate is believed to be changing, and new patterns are emerging, models are created to represent future climate predictions. The models are referred to as Atmosphere-Ocean Global Climate Models. These models are made up of complex mathematical models and equations that represent climate variables, and can be used to predict future climatic events. AOGCMs are discussed further in section 3.2.2.

1.3 Statistical Tools

With new ideas about more appropriate distributions emerging, studies must be done to ensure we are using the most accurate method available. Findings in this report will shed more light onto the accuracy of the currently accepted methods, and will compare the benefits of a new distribution. The three distributions compared are the Generalized Extreme Value (GEV), Log-Pearson type 3 (LP3), and Gumbel (EV1). LP3 and GEV are 3 parameter distributions, compared to EV1, which only uses 2 parameters. Since 1967, the U.S Water Resource Council has recommended and required the use of LP3 distributions for all U.S analysis. This has recently been called into question by several papers in the U.S that have done similar studies as carried out in this report, which have

found that the GEV distribution is an acceptable distribution, and often preferred over LP3 (Vogel, 1993). In Canada, the current required distribution for Precipitation Analysis is EV1 used with the method of moments (MOM), as determined by Environment Canada (EC Gumbel). Similar to the U.S, recent studies have been carried out to investigate the use of GEV distribution in the Canadian context. A study from Saskatchewan (Nazemi, 2011) investigated the use of GEV for the city of Saskatoon, finding that the GEV model is viable, however more studies need to be conducted to determine the appropriate use of the shape parameter as it greatly affected the results.

1.4 Objective of the Study

The main objective of this report is to investigate the differences between three common statistical distributions used in Precipitation Analysis. As the climate is changing, the necessity to accurately estimate extreme events plays an important role in climatology. This report will investigate the goodness of fit of the GEV, EV1 and LP3 distributions with respect to Upper Thames River Watershed, using data collected from the London International Airport Station under climate change.

This study will also calculate Intensity Duration Frequency curves with the data, which estimate the future extreme precipitation events, which are necessary for design purposes.

1.5 Research Procedure

The appropriateness of the distributions is investigated by the goodness of fit tests and the L-Moment Ratio Diagrams. For goodness of fit tests, the Anderson-Darling (AD), the Kolmogorov-Smirnov (KS), and the Chi-Squared tests were used in this report. The shape parameter of the GEV distribution was also analyzed, which provides more insight into the goodness of fit of the distribution.

There are several methods available to estimate the parameters of these distributions. The method of L-Moments which is very often used in hydrology studies is applied in this report for the estimation of GEV, LP3 and EV1 parameters.

1.6 Organization of the Report

This report comprises of 4 sections. Section 2 will explain the statistical theory and all methodology used in the estimation LP3, GEV and EV1 parameters, as well as the advantages/disadvantages of each distribution. The goodness of fit tests used in the report are also described in this section, as well as a brief section about Intensity Duration Frequency curves. The study area of The Upper Thames River Basin is described in section 3, along with the input data and discussion of the results of the goodness of fit tests. The report concludes in section 4.

2. Methodology

2.1 Statistical Distributions

The GEV, EV1 and LP3 distributions used in this report have a wide variety of applications for estimating extreme values of given data sets. They are commonly used in hydrological applications. The following sections will explain and compare the theory of the distributions, as well describe the advantages and disadvantages of each.

2.1.1 Generalized Extreme Value Distribution (GEV)

The GEV distribution is a family of continuous probability distributions that combines the Gumbel (EV1), Frechet and Weibull distributions. GEV makes use of 3 parameters: location, scale and shape. The location parameter describes the shift of a distribution in a given direction on the horizontal axis. The scale parameter describes how spread out the distribution is, and defines where the bulk of the distribution lies. As the scale parameter increases, the distribution will become more spread out. The 3rd parameter in the GEV family is the shape parameter, which strictly affects the shape of the distribution, and governs the tail of each distribution. The shape parameter is derived from skewness, as it represents where the majority of the data lies, which creates the tail(s) of the distribution. When shape parameter (k)=0, this is the EV1 distribution. When $k>0$, this is EV2 (frechet), and when $k<0$ is the EV3 (Weibull).

A large problem in working with the Extreme Value distributions is determining whether to use Type 1, 2 or 3. EV3, which has a negative shape parameter is often appealing as it has a finite upper limit, which the general belief of observed flood magnitudes (Cunnane, 1989). In general, a distribution with a larger number of flexible parameters, for instance GEV, will be able to model the input data more accurately than a distribution with a lesser number of parameters. EV1 is effective for small sample sizes, however if the size is greater than 50, GEV shows a better overall performance (Cunnane, 1989). This report investigates the truth of these statements by analyzing the goodness of fit of these distributions in chapter 3.

When recreating synthetic data from a sample data set and finding return values using data fit to the GEV distribution, the results have less bias than data fit to the Gumbel distribution. Results from (Cunnane, 1989) show that distributions with 2 parameters (EV1) have smaller standard error, but larger bias than 3 or 4 parameter distributions (GEV, LP3), especially in a small sample size. The 3 or 4 parameter distributions often have negligible bias.

As stated in the introduction, the shape parameter for GEV can greatly affect the results. A positive shape parameter will result in the distributions being upper bounded. This phenomenon is undesirable in practical applications as this produces very minimal differences in magnitudes between large return periods. A negative shape parameter assures that the distribution is unbounded and that results in an increase in magnitudes, as the return period gets larger. When designing for extreme events, we are looking for these large values.

The CDF and PDF are defined in (Hosking, 1997) as:

$$F(x) = \exp \left\{ - \left(1 - \frac{\kappa(x-\xi)}{\alpha} \right)^{1/\kappa} \right\} \quad (2.1)$$

$$f(x) = \alpha^{-1} \exp \left[- (1 - \kappa)y - \exp(-y) \right] \quad (2.2)$$

where $y = -\kappa^{-1} \log \left[1 - \frac{\kappa(x-\xi)}{\alpha} \right]$, when $\kappa \neq 0$

where, ξ is the location parameter, α is the scale parameter, and κ is the shape parameter.

2.1.2 Gumbel Distribution (EV1)

The EV1 distribution only uses 2 parameters, location (ξ) and scale (α). This is the current required method for all Precipitation Frequency Analysis in Canada.

The CDF and PDF as defined in (Hosking, 1997) are:

$$F(x) = \exp \left[- \exp \left(- \frac{x-\xi}{\alpha} \right) \right] \quad (2.3)$$

$$f(x) = \alpha^{-1} \exp \left(- \frac{x-\xi}{\alpha} \right) \exp \left[- \exp \left(- \frac{x-\xi}{\alpha} \right) \right] \quad (2.4)$$

where, ξ is the location parameter, α is the scale parameter

2.1.3 Log Pearson Type 3 Distribution (LP3)

The LP3 distribution is a member of the family of Pearson Type 3 distributions, and is also referred to as the Gamma distribution. This is the current required method to be used for all Precipitation Frequency Analysis in the United States. The LP3 distribution is complicated, as it has 2 interacting shape parameters (Stedinger, 2007). Similar to GEV it uses 3 parameters, location (μ), scale (σ) and shape (γ). A problem arises with LP3 as it has a tendency to give low upper bounds of the precipitation magnitudes, which is undesirable (Cunnane, 1989).

The CDF and PDF are defined in (Hosking, 1997) as:

If $\gamma \neq 0$, let $\alpha = 4/\gamma^2$ and $\xi = \mu - 2\sigma/\gamma$

If $\gamma > 0$, then

$$F(x) = G\left(\alpha, \frac{x-\xi}{\beta}\right)/\Gamma(\alpha) \quad (2.5)$$

$$f(x) = \frac{(x-\xi)^{\alpha-1} e^{-(x-\xi)/\beta}}{\beta^\alpha \Gamma(\alpha)} \quad (2.6)$$

if $\gamma = 0$ the distribution is Normal and

$$F(x) = \Phi\left(\frac{x-\mu}{\sigma}\right) \quad (2.7)$$

$$f(x) = \phi\left(\frac{x-\mu}{\sigma}\right) \quad (2.8)$$

if $\gamma < 0$, then

$$F(x) = 1 - G\left(\alpha, \frac{\xi-x}{\beta}\right)/\Gamma(\alpha) \quad (2.9)$$

$$f(x) = \frac{(\xi-x)^{\alpha-1} e^{-(\xi-x)/\beta}}{\beta^\alpha \Gamma(\alpha)} \quad (2.10)$$

where μ is the location parameter, σ is the scale parameter, and γ is the shape parameter. For more information refer to (Hosking, 1997) page 200.

2.2 Parameter Estimation Techniques

A common statistical tool to estimate distribution parameters is to use maximum likelihood estimators or method of moments (MOM). Environment Canada uses, and recommends the MOM technique to estimate the parameters for EV1. Another method of estimation is the method of L-Moments, which will be used in this report to calculate the parameters of the GEV distribution. L-Moments are based on probability-weighted moments (PWMs), however provide a greater degree of accuracy and ease. PWMs use weights of the cumulative distribution function (F), however it is difficult to interpret the moments as scale and shape parameters for probability distributions (Hosking, 1997). L-Moments are a modification of the PWMs, as they use the PWMs to calculate parameters that are easier to interpret and that can be used in the calculation of parameters for statistical distributions. L-Moments are based on linear combinations of data that have been arranged in ascending order. They provide an advantage, as they are easy to work with, and more reliable as they are less sensitive to outliers. The method of L-Moments calculates more accurate parameters than the MOM technique for smaller sample sizes. (Kochanek, 2010) The MOM techniques only apply to a limited range of parameters, whereas L-Moments can be more widely used, and are also nearly unbiased (Rowinski, 2001).

2.2.1 Probability Weighted Moments Equations

PWMs are needed for the calculation of L-Moments. The data first must be arranged in ascending order, and then apply the following equations from (Cunnane, 1989).

$$M_{100} = \text{sample mean} = \frac{1}{N} \sum_{i=1}^N Q_i \quad (2.11)$$

$$M_{110} = \frac{1}{N} \sum_{i=1}^N \frac{(i-1)}{(N-1)} Q_i \quad (2.12)$$

$$M_{120} = \frac{1}{N} \sum_{i=1}^N \frac{(i-1)(i-2)}{(N-1)(N-2)} Q_i \quad (2.13)$$

$$M_{130} = \frac{1}{N} \sum_{i=1}^N \frac{(i-1)(i-2)(i-3)}{(N-1)(N-2)(N-3)} Q_i \quad (2.14)$$

in which N is the sample size, Q is the data value, and i is the rank of the value in ascending order.

2.2.2 L-Moment Equations

The following L-Moments are defined in (Cunnane, 1989):

$$\lambda_1 = L1 = M_{100} \quad (2.15)$$

$$\lambda_2 = L2 = 2M_{110} - M_{100} \quad (2.16)$$

$$\lambda_3 = L3 = 6M_{120} - 6M_{110} + M_{100} \quad (2.17)$$

$$\lambda_4 = L4 = 20M_{130} - 30M_{120} + 12M_{110} - M_{100} \quad (2.18)$$

The 4 L-Moments ($\lambda_1, \lambda_2, \lambda_3, \lambda_4$) are all derived using the 4 PWMs. Other useful ratios are L-CV (τ_2), L-Skewness (τ_3) and L-Kurtosis (τ_4).

L-CV is similar to the normal coefficient of variation (CV). The standard equation for $CV = \frac{\text{Standard Deviation}}{\text{Mean}}$, and shows how the data set varies. The larger the CV value, the larger the variation of the data set from the mean. For example, in arid regions that receive few storm events, the variation will be large, as one storm will deviate greatly from the low mean.

$$\tau_2 = L2/L1 \quad (\text{L-CV}) \quad (2.19)$$

L-Skewness is a measure of the lack of symmetry in a distribution. If the value is negative, the left tail is long compared with the right tail, and if the value is positive, the right tail is longer. For GEV frequency analysis, a positive L-Skewness value is desired, as we are interested in the extreme events that occur in the right side tail of the distribution.

$$\tau_3 = L_3/L_2 \quad (\text{L-Skewness}) \quad (2.20)$$

L-Kurtosis is difficult to interpret, however is often described as the measure of “peakedness” of the distribution (Hosking, 1997). L-kurtosis is much less biased than ordinary kurtosis.

$$\tau_4 = L_4/L_2 \quad (\text{L-Kurtosis}) \quad (2.21)$$

2.2.3 Generalized Extreme Value

As stated, the GEV distribution uses three parameters: ξ is the location parameter, α is the scale parameter and κ is the shape parameter. The parameters are defined from (Hosking, 1997) as:

$$\kappa = 7.8590c + 2.9554c^2 \quad (2.22)$$

$$\text{in which } c = \frac{2}{3 + \tau_3} - \frac{\ln 2}{\ln 3}$$

$$\alpha = \frac{\lambda_2 k}{(1 - 2^{-k})\Gamma(1 + k)} \quad (2.23)$$

$$\xi = \lambda_1 - \alpha\{1 - \Gamma(1 + k)\}/k \quad (2.24)$$

in which Γ = the gamma function

Once all parameters have been estimated, calculating the T-year Return Precipitation (Q_t) can be done using:

$$Q_t = \xi + \left(\frac{\alpha}{k}\right) \left\{1 - \left(-\log\left(\frac{T-1}{T}\right)\right)^k\right\} \quad (2.25)$$

in which T is the desired return period in years.

Although there are several computer programs capable of working with the GEV distribution, all calculations were done in excel using basic macros and formulas. For reference, the following is a simple step-by-step procedure for the estimation of the GEV parameters.

Step by step GEV

- i. sort the data set by ordering all of the data points in ascending order (lowest to highest)
- ii. calculate the 4 PWM's ($M_{100}, M_{110}, M_{120}, M_{130}$)
- iii. calculate the 4 L-Moments ($\lambda_1, \lambda_2, \lambda_3, \lambda_4$) using the PWMs
- iv. calculate k, the shape parameter
- v. calculate ξ , the location parameter and α , the scale parameter
- vi. using the desired return period, apply all parameters to the Return Period equation to calculate the estimated return value

2.2.4 Gumbel (EV1)

The EV1 Parameters are defined in (Hosking, 1997):

$$\alpha = \frac{\lambda_2}{\log 2} \quad (2.26)$$

$$\xi = \lambda_1 - (\alpha\gamma) \quad (2.27)$$

in which $\gamma = 0.5772$ (Euler's Constant)

$$Q_t = \xi + \alpha y_t, \quad (2.28)$$

$$\text{in which } y_t = -\ln \left[-\ln \left(1 - \left(\frac{1}{T} \right) \right) \right] \quad (2.29)$$

where T is the return period in years.

2.2.5 Log Pearson Type 3

The LP3 parameters are defined in (Hosking, 1997):

$$\gamma = 2\alpha^{-0.5} \text{sign}(\tau_3) \quad (2.30)$$

$$\sigma = \frac{\lambda_2 \pi^{0.5} \alpha^{0.5} \Gamma(\alpha)}{\Gamma(\alpha+0.5)} \quad (2.31)$$

$$\mu = \lambda_1 \quad (2.32)$$

for estimating α ;

if $0 < |\tau_3| < \frac{1}{3}$, let $z = 3\pi\tau_3^2$ and use

$$\alpha = \frac{1+0.2906z}{z+0.1882z^2+0.0442z^3} \quad (2.33)$$

if $\frac{1}{3} < |\tau_3| < 1$, let $z = 1 - |\tau_3|$ and use

$$\alpha = \frac{0.36067z-0.59567z^2+0.25361z^3}{1-2.78861z+2.56096z^2-0.77045z^3} \quad (2.34)$$

2.3 Goodness of Fit tests

Goodness of fit tests can be reliably used in climate statistics to assist in finding the best distribution to use to fit the given data. These tests cannot be used to pick the best distribution, rather to reject possible distributions. These tests calculate test-statistics, which are used to analyze how well the data fits the given distribution. These tests describe the differences between the observed data values, and the expected values from the distribution being tested.

The Anderson-Darling (AD), Kolmogorov-Smirnov (KS), and Chi-Squared (χ^2) tests were used for the goodness of fit tests in this report. All test statistics are defined in (Solaiman, 2011).

The goodness of fit tests were executed in the downloadable software EasyFit, available at <http://www.mathwave.com/easyfit-distribution-fitting.html>. All test values and statistics were produced from this program.

2.3.1 Anderson-Darling Test

The Anderson-Darling test compares an observed CDF to an expected CDF. This method gives more weight to the tail of the distribution than KS test, which in turn leads to the AD test being stronger, and having more weight than the KS test. The test rejects the hypothesis regarding the distribution level if the statistic obtained is greater than a critical value at a given significance level (α). The significance level most commonly used is $\alpha=0.05$, producing a critical value of 2.5018. This number is then compared with the test distributions statistic to determine if it can be rejected or not. The AD test statistic (A^2) is:

$$A^2 = -n - \frac{1}{n} \sum_{i=1}^n (2i - 1) \cdot [\ln F(x_i) + \ln(1 - F(x_{n-i+1}))] \quad (2.35)$$

2.3.2 Kolmogorov-Smirnov Test

The Kolmogorov-Smirnov test statistic is based on the greatest vertical distance from the empirical and theoretical CDFs. Similar to the AD test statistic, a hypothesis is rejected if the test statistic is greater than the critical value at a chosen significance level. For the significance level of $\alpha=0.05$, the critical value calculated is 0.12555. The samples are assumed to be from a CDF $F(x)$. The test statistic (D) is:

$$D = \max\left(F(x_i) - \frac{i-1}{n}, \frac{i}{n} - F(x_i)\right) \quad (2.36)$$

2.3.3 Chi-Squared Test

The Chi-Squared test is used to determine if a sample comes from a given distribution. It should be noted that this is not considered a high power statistical test and is not very useful (Cunnane, 1989). The test is based on binned data, and the number of bins (k) is determined by:

$$k = 1 + \log_2 N \quad (2.37)$$

in which N= sample size

The test statistic (χ^2) is:

$$\chi^2 = \sum_{i=1}^k \frac{(O_i - E_i)^2}{E_i} \quad (2.38)$$

where,

O_i is the observed frequency

E_i is the expected frequency, $E_i = F(x_2) - F(x_1)$

where x_1 and x_2 are the limits of the i^{th} bin

The significance level, $\alpha=0.05$ produced a critical value of 12.592 which is used in this report. Again, if the test statistic is greater than the critical value, the hypothesis is rejected.

2.3.4 L-Moment Ratio Diagrams

Another way to measure goodness of fit is to construct an L-Moment Ratio Diagram. This is a diagram of L-Skewness and L-Kurtosis of the sample data set, which is plotted against constant lines and points of known statistical distributions of interest. This is a common technique used in Regional Flood Frequency Analysis, which uses the average values of L-Skewness and L-Kurtosis from several stations in an area. The goodness of fit for the observed data is determined by comparing the values against the fitted regional data. In this report, there was no regional data to use for averages and comparison, as only data from one station was analyzed. However the use of L-Moment ratio diagrams

can still be used in this context for comparing the observed data against the 3 known distributions of interest; GEV, Gumbel and LP3.

Many statistical distributions have predetermined relationships between L-Skewness and L-Kurtosis (τ_3 and τ_4). These are useful and necessary for creating L-Moment Ratio Diagrams, to visually inspect which distribution has the best fit. As EV1 is a 2-parameter distribution with only location and scale parameters, this plots as a single point with a constant τ_3 value of 0.1699, and a τ_4 value of 0.1504. Parameters differing only in scale and location have by definition the same values of L-Kurtosis and L-Skewness. Three parameter distributions (GEV, LP3) are plotted as a line that corresponds to the varying shape parameters. The expressions for τ_4 are given as functions of τ_3 and are approximated as follows (Hosking and Wallis 1997).

LP3

$$\tau_4 = 0.1224 + 0.30115\tau_3^2 + 0.95812\tau_3^4 - 0.57488\tau_3^6 + 0.19383\tau_3^8$$

GEV

$$\tau_4 = 0.10701 + 0.1109\tau_3 + 0.84838\tau_3^2 - 0.06669\tau_3^3 + 0.00567\tau_3^4 - 0.04208\tau_3^5 + 0.03673\tau_3^6$$

Step by Step L-Moment Diagrams

- i. create a table containing L-Skewness and L-Kurtosis values for each data set (in this case 27 sets for each AOGCM)
- ii. plot L-Skewness against L-Kurtosis of the observed data sets
- iii. plot L-Skewness against L-Kurtosis of the given distributions, and visually compare the plot

2.4 Intensity Duration Frequency Curves & Storm Durations

The purpose of fitting data to statistical distributions is to be able to estimate the probability of extreme precipitation intensities for a given return period (T). Firstly, the

maximum amount of precipitation for a given storm duration is calculated (P_t), and is then converted into an intensity (commonly with units of mm/hour). This intensity value is needed for many design calculations, most commonly for determining peak flow or peak runoff. The estimated return values are needed to construct Intensity Duration Frequency curves (IDF curves), which are widely used in engineering applications. These curves show the relationship between the intensity of the precipitation and the duration of the storm for a given return period. The IDF curves are developed for a specific location, with a specific return period. IDF curves developed in this report are shown in section 3.4.2.

The P_t , or IDF curve value is the design precipitation that has the probability of occurring on average $1/T$ for each year. For example, if the P_t value for a 100-year return period, for a 1-hour storm duration is 100mm, there is a $1/100$ (1%) chance of this extreme precipitation value occurring in any given year.

Estimating design floods plays an important role in the planning and management of floodplains. Planning for design floods does not guarantee that the area will be protected for the amount of years designed for, however it is a safety measurement that must be met, and the return period varies depending on various requirements. In this report, the design precipitation value is calculated, which is needed to estimate the design flood. The design flood is calculated using many factors such as the ground type (imperviousness), slope, vegetation and of course precipitation intensity. The precipitation intensity is determined from IDF curves, which are shown in chapter 2 of this report.

2.4.1 Storm Durations

Determining precipitation intensities for various storm lengths is an important aspect for safely designing structures and infrastructure to manage flooding. Often short storm durations are desired as they can give high intensities (mm/hr). The data sets in this report were initially given in total daily precipitation, that is 365 data points for each year. A disaggregation technique was used to break the data down into hourly time steps, which

is 24 data points for each day. To determine the 1-hour annual maximum, each day of the year is disaggregated into hourly data to produce a total of 8,760 data points (365x24). The maximum value of this data set is the 1-hour annual maximum precipitation. This was done for all 117 years of data created to produce the annual maximum data series, which is necessary to use in the statistical distributions in this report. Storm durations of 1, 2, 6, 12 and 24 hours were used for this report. The longer storm durations were all created using combinations of the hourly precipitation data. For example, the 2-hour storm used 4,380 (365x12) data points for each year to determine the 2-hour annual maximum series.

3. Case Study

3.1 Study Area: The Upper Thames River Watershed

The Upper Thames River Watershed (UTRW) is located between Lake Huron and Lake Erie in Southwestern Ontario, and has an area of 3842 km². The watershed is largely comprised of rural areas, however it is home to approximately 485,000 people, mostly in the main centers of London, Stratford and Woodstock. London alone is home to approximately 350,000 residents, many of whom experience the affects of flooding as the Thames River runs directly through he city (UTRCA, 2011). The Thames River is quite large, with a total length of 273 km and an average annual discharge of 35.9 m³/s (Prodanovic, 2006). The UTRW receives approximately 1,000 mm of annual precipitation, however 60% of this is lost due to mechanisms including evaporation and evapotranspiration. The Thames River has experienced several extreme flood events, most recently in July 2000, April 2008 and December 2008.

The UTRW contains 6 weather-gauging stations, with 9 more in the surrounding area. The station used in this study is the London International Airport, with latitude of 43.03° N, longitude 81.16° W and an elevation of 278 m above sea level.

3.2 Input Data

All historical and climate model data sets used in this report have been collected and processed for a PhD thesis (Solaiman, 2011). For detailed information on all data collected, including downscaling techniques and the application of all global climate models, please refer to the PhD thesis.

3.2.1 Historical Data

This report uses daily precipitation data collected from the UTRW for a period of 39 years from 1965-2003, from the London International Airport Station. The observed historical data has been collected from Environment Canada (National, 2011) and

simulated using 11 different climate models, each with a number of various emission scenarios.

3.2.2 Data Manipulation

The observed data was simulated in the WG-PCA weather generator to produce the various data sets for the application of the statistical distributions (Solaiman, 2011). Weather generators are used to generate long sequences of daily precipitation data for various climate models, also known as Atmosphere-Ocean Global Climate Models (AOGCM).

Weather generators are essentially random number generators, and are also capable of producing a synthetic data set with the same, or when using AOGCMs, different, statistical properties of the input data. The observed historical data from the London International Airport station was simulated in the weather generator, using both perturbed (different maximum and minimum values) and unperturbed (same maximum and minimum values as input data) settings. These techniques are useful for researchers as this enables them to account for natural environmental variability, while keeping almost identical distribution parameters. The simulation of the 39 years of data was done 3 times, to create a total of 117 years of synthetic historical data, sufficient enough for the estimation of a 100-year return period which is a common design period. (Solaiman, 2011)

AOGCMs are complex mathematical models of the atmosphere and the ocean that combine rotating sphere and thermodynamic equations using various energy sources. They are often the key component in computer programs that model the atmospheric or ocean conditions of the Earth. AOGCMs are also used in weather forecasting and have many applications in investigating and predicting climate change. The models are used in this report to produce various precipitation data sets that can be fitted to the three distributions being analyzed. The wide range of models used accounts for variability in the future climate data, however the actual values produced are not of importance in the context of this report. The models were needed to provide a large amount of data to test

with the distributions to determine which has the most appropriate fit. These models also have various scenarios that can be applied to them, which vary in future emissions, economic and population predictions, which all having varying effects on the future climate. These global models are not designed for local modeling however, so a downscaling method must be used. Downscaling of the AOGCMs is done to convert these large-scale models into the scale in question, and is done using the K-nearest neighbor approach. Weights are calculated by comparing the new data to the historical data, calculating a correction ratio to be applied. For more information on the downscaling and data processing, refer to (Solaiman, 2011).

Once the 117 years of synthetic data were created, the weather generator was again used to simulate the data under 11 different AOGCMs with various emission scenarios, thus creating a total of 27 different data sets.

3.2.3 Description of AOGCM Models

Table 3.1 shows the 11 AOGCMs used, with the combination of the 3 available emission scenarios that were applied to each model. The CGCM3T models were created by the Canadian Centre for Climate Modeling and Analysis for the IPCC in 2005. The models use 4 major components: an ocean global climate model, an atmospheric global climate model, a thermodynamic sea-ice model, and a land surface model. The CSIRO-Mk models were created by Australia's Commonwealth Scientific and Industrial Research Organization, and consist of atmosphere, land surface and ocean and polar ice components. Max Planck Institute for Meteorology created the ECHAM model, which is capable of hosting sub-models beyond the processes of an AOGCM. The ECHO-G model is coupled, using the ECHAM atmospheric model, along with the HOPE ocean model, and was created by the University of Bonn Meteorological Research Institute of KMA. The Goddard Institute for Space Studies, along with NASA, developed the GISSAOM model in 1995, and was edited in 2004. The Japanese Model for Interdisciplinary Research on Climate developed a high-resolution model, MIROC3-HIRES, and a medium resolution model, MIROC3-MEDRES. The CCSRNIES and GFDL-CM2.1 models are both used by the IPCC and consist of coupled models.

3.2.4 Emission Scenarios

All scenario information is from (Nakicenovic et al, 2000).

A1B: This scenario uses the assumption of rapid economic expansion and globalization, a total population of 9 billion in 2050, and a wide range of energy sources.

B1: This scenario is similar to A1B, however it presumes a more resource efficient world, with the use of clean technologies and emphasis on global sustainability.

A2: This scenario consists of a world of independent nations, with an increasing population, with slower technological advancements.

Model	Emission scenarios
CCSRNIES	B21
CSIROMK2b	B11
CSIROMK35	A1B, B1, A2
CGCM3T47	A1B, B1, A2
CGCM3T63	A1B, B1, A2
ECHAM5AOM	A1B, B1, A2
ECHO-G	A1B, B1, A2
GFDLCM2.1	A1B, B2, A2
GISSAOM	A1B, B1
MIROC3HIRES	A1B, B1
MIROC3MEDRES	A1B, B1, A2

Table 3.1: Summary of AOGCMs and emission scenarios

3.3 Results

In this section the results for the goodness of fit tests and the L-Moment ratio diagrams are discussed with respect to the statistical distributions in question. In both tests, for all storm durations the GEV distribution appears to have the most appropriate fit.

3.3.1 Goodness of Fit Tests

Combining the 27 data sets produced from the AOGCM's, and the 5 different storm duration data, a total of 135 data sets were used in the goodness of fit tests. For the purpose of this report, each testing method only compared the three distributions discussed: GEV, LP3 and EV1. The test results were calculated using the methods described in chapter 2.3 of the report. Analyzing the goodness of fit results is a way to determine which of the distributions should not be considered, if there is a clear trend in the results. These tests do not provide a simple yes or no answer to whether the distribution should be used, and must be considered with other test methods (L-Moment Ratio Diagrams).

The GEV distribution showed to have the best fit of the 3 distributions. Out of the 135 data sets, the Kolmogorov-Smirnov test results did not reject GEV distribution in any circumstance. The Anderson-Darling test also did not reject the GEV distribution at all. The Chi-squared method rejected GEV least frequently of the 3 distributions, with a total of 14 (10.4% of the time).

The LP3 distribution showed to fit the second best. Similar to GEV, the Kolmogorov-Smirnov test also did not reject LP3 at all. The Anderson-Darling test rejected LP3 a total of 8 times (6% of the time), and Chi-Squared test rejected LP3 22 times (16.3% of the time).

The EV1 distribution showed to have the worst fit as it was rejected 11 times by Kolmogorov-Smirnov, 20 times by Anderson-Darling and 37 times by Chi-Squared.

	GEV	LP3	EV1
Kolmogorov-Smirnov	0	0	11
Anderson-Darling	0	8	20
Chi-Squared	14	22	37

Table 3.2: Number of rejections at the 5% significance level for the 3 goodness of fit tests

These results show that in comparison to EV1, the GEV distribution is a more acceptable fit for the data used from the London International Airport station.

3.3.2 L-Moment Ratio Diagrams

L-Moment Ratio Diagrams were constructed for each of the 5 storm durations, as well as the historical unperturbed data using the methodology discussed in chapter 2.3 of the report. Figure 3.2 displays the 12-hour L-Moment ratio diagram, with all 27 data points from each scenario shown. Diagrams of other storm durations can be located in the appendix. The average of the 27 scenarios is shown (red square), as well as the base distributions for comparison of GEV, EV1 and LP3. The EV1 distribution is shown as a single point (green triangle). Figure 3.1 shows the data for the 12-hour storm follows the GEV distribution very well. The diagrams shown in the appendix all display very similar results to figure 3.1 and show that the GEV distribution has the best fit when analyzing L-Moment Ratio Diagrams for the London International Airport Station data.

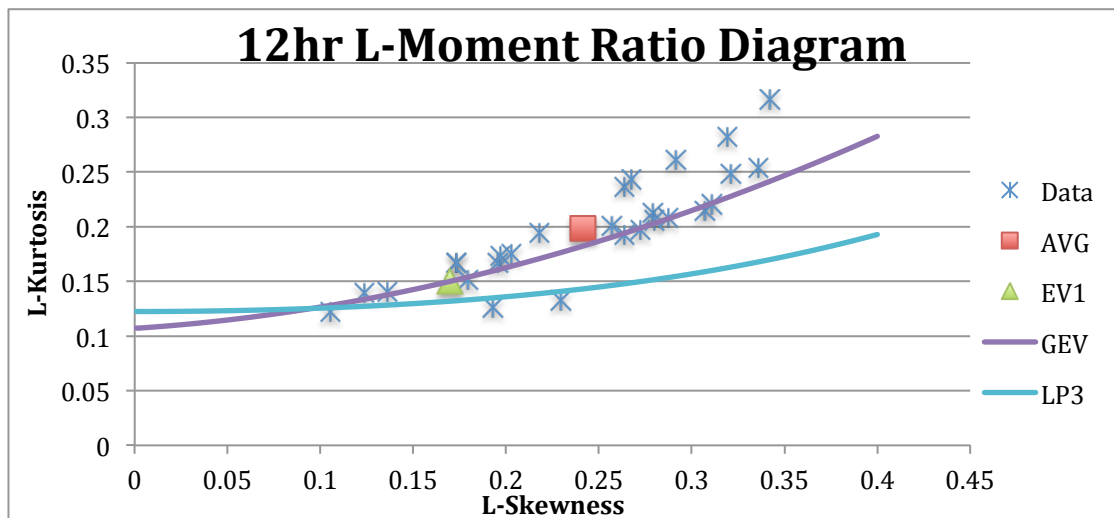


Figure 3.1: L-Moment Ratio Diagram for 12-hour storm duration

3.3.3 Shape Parameter

As discussed in section 2.1.1, the shape parameter determines the shape of the distribution. A negative value determines that the distribution is upper unbounded, and a positive value leads to the distribution being upper bounded. This is why even if the data is a good fit to the GEV distribution, if the shape parameter is positive, this may be undesirable in practical applications. Therefore an evaluation of the shape parameter for all data sets is needed, and is performed in this section.

Table 3.3 lists the shape parameter values for all AOGCM data sets for the 5 different storm durations.

Analyzing the parameters from all data sets used in the report shows that the average κ -value is -0.108 with only 23 positive values of the 135 data sets. It should also be noted that the positive values are all very close to 0, further displaying the suitability of the GEV in this context

AOGCM	Storm Duration (hours)				
	<i>1</i>	<i>2</i>	<i>6</i>	<i>12</i>	<i>24</i>
<i>CCSRNIES B21</i>	-0.1212	-0.2476	-0.2494	-0.1415	-0.0603
<i>CSIROMK2b B11</i>	-0.0762	-0.1863	-0.2307	-0.1640	-0.1227
<i>CGCM3T47 A1B</i>	0.0151	-0.1155	-0.2635	-0.1541	-0.1653
<i>CGCM3T47 B1</i>	-0.0415	-0.0220	-0.0350	-0.0739	-0.1438
<i>CGCM3T47 A2</i>	-0.1371	-0.1134	-0.2593	-0.2234	-0.2059
<i>CGCM3T63 A1B</i>	-0.1167	-0.2985	-0.3280	-0.2035	-0.1396
<i>CGCM3T63 B1</i>	-0.0925	-0.2849	-0.3006	-0.1816	-0.1939
<i>CGCM3T63 A2</i>	0.0642	-0.1379	-0.2116	-0.0055	0.0464
<i>CSIROMK35 A1B</i>	0.0188	0.0566	-0.0942	-0.0999	-0.1103
<i>CSIROMK35 B1</i>	-0.0298	-0.0106	-0.0561	-0.0911	-0.1057
<i>CSIROMK35 A2</i>	-0.1025	-0.0547	-0.1176	-0.1415	-0.1213
<i>ECHAM5AOM A1B</i>	-0.1609	-0.1814	-0.1979	-0.1756	-0.1467
<i>ECHAM5AOM B1</i>	0.0311	-0.0999	-0.0710	0.0739	0.1037
<i>ECHAM5AOM A2</i>	0.0193	-0.1214	-0.1155	-0.0355	-0.0606
<i>ECHO-G A1B</i>	0.0167	-0.1222	-0.2086	-0.2207	-0.2338
<i>ECHO-G B1</i>	-0.1152	-0.1969	-0.1712	-0.1647	-0.1375
<i>ECHO-G A2</i>	-0.0977	-0.1610	-0.1448	-0.0400	-0.0287

<i>GFDLCM2.1 A1B</i>	-0.0357	-0.0330	0.0243	0.1035	0.0974
<i>GFDLCM2.1 B1</i>	-0.2069	-0.1719	-0.2506	-0.2526	-0.2059
<i>GFDLCM2.1 A2</i>	0.0001	-0.1495	-0.1513	-0.1320	-0.0969
<i>GISSAOM A1B</i>	-0.0184	-0.2196	-0.3029	-0.2092	-0.1499
<i>GISSAOM B1</i>	0.0974	-0.1213	-0.1673	-0.0422	-0.0213
<i>MIROM3HIRES A1B</i>	0.0008	0.0011	0.0067	0.0536	0.0040
<i>MIROM3HIRES B1</i>	0.0031	-0.1628	-0.2335	-0.1468	-0.0851
<i>MIROC3MEDRES A1B</i>	-0.1128	-0.1625	-0.2232	-0.2441	-0.1704
<i>MIROC3MEDRES B1</i>	0.0172	-0.0870	-0.0458	-0.0512	0.0141
<i>MIROC3MEDRES A2</i>	-0.1570	-0.0412	-0.0313	-0.0148	-0.0071

Table 3.3: Shape Parameter values for all AOGCM data sets

Figure 3.2 displays the boxplot for the shape parameter for all 5 storm durations. This shows how the shape parameter values vary for each of the data sets. The minimum, first quartile, median, third quartile and maximum values are all represented in the figure, and gives a very good indication of the negative trend in the data. The mean and median of the 5 different storm durations are all negative, which is desired for the practical application of the GEV distribution. The 6-hour storm duration has the most negative values, with a median value of -0.1693. The 1-hour storm duration has the least negative median of -0.0328. The most negative value is from the 6-hour duration and is -.02415, and the largest value is from the 24-hour duration with 0.1037.

Table 3.4 displays the quartile information used for the boxplot in figure 3.2. These values display the negative trend for the shape parameter of all the data sets.

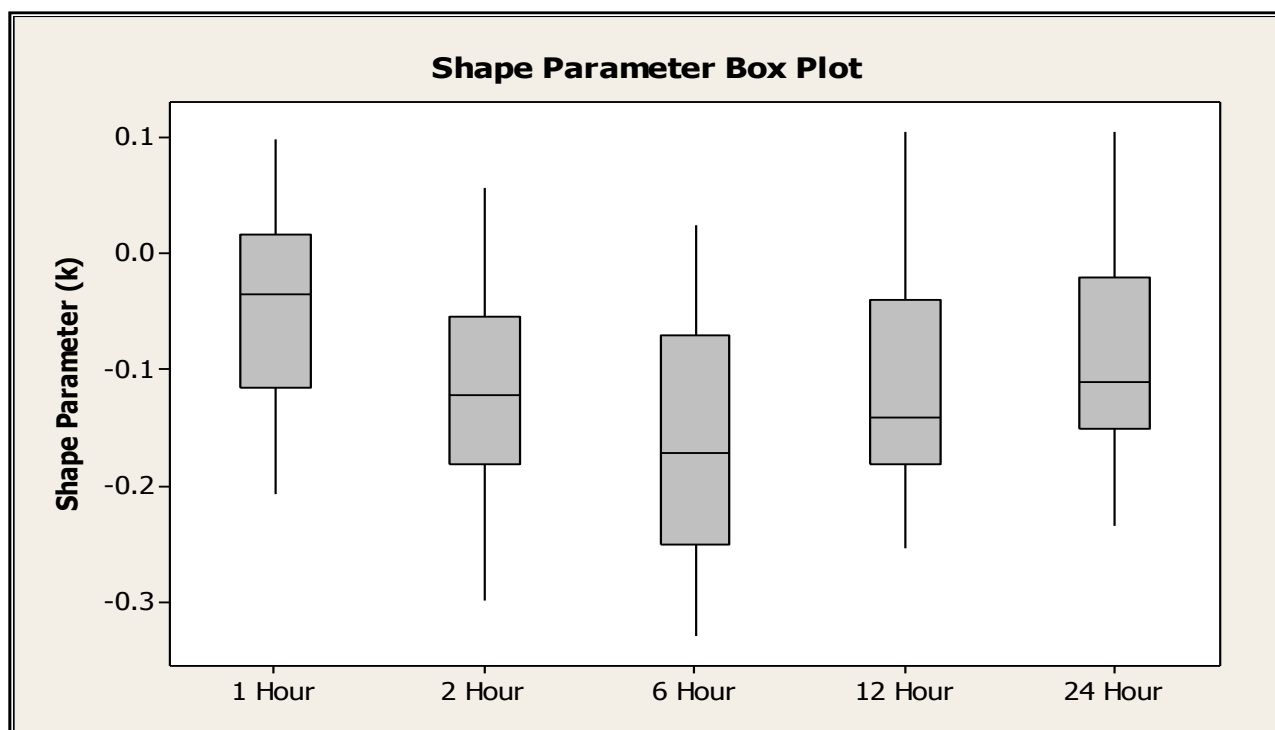


Figure 3.2: Boxplot of shape parameter values for all 5 storm durations

Quartile	Storm Duration (hours)				
	1	2	6	12	24
<i>q1</i>	-0.1140	-0.1767	-0.2415	-0.1786	-0.1483
<i>median</i>	-0.0328	-0.1218	-0.1693	-0.1367	-0.1158
<i>q3</i>	0.0163	-0.0628	-0.0768	-0.0405	-0.0232
<i>min</i>	-0.2069	-0.2985	-0.3280	-0.2526	-0.2338
<i>max</i>	0.0974	0.0566	0.0243	0.1035	0.1037

Table 3.4: Summary of quartile information for shape parameter boxplot

Refer to the appendix for graphs of the variation of the shape parameter with respect to each AOGCM.

3.4 GEV Return Values & Uncertainties

For the context of this report, the return values are of little importance. The goal was not to determine the accuracy of these values, rather to discuss the fit of each distribution as done in section 3.3. When using data from different AOGCMs, it is believed that a very large amount of uncertainty is included in the estimation of IDF curve for future climate. By making use of all data produced by the 27 different scenarios, the many variations of climate change encompassing all uncertainties were taken into account, which gave a wide variety of results to analyze. The following pages discuss the differences between the results between the models used, as well as the historical data from Environment Canada. They show that there is a clear need for more studies done on the GEV distribution, as the results can be significantly different in comparison to current Environment Canada standards which use the EV1 distribution.

After analyzing all 27 models, the emission scenario that produced the most intense (wet) results was ECHAM5AOM_A1B, and the least intense scenario (dry) was MIROC3MEDRES_A2. The data in table 3.3 shows the depth of rain in mm for each return period, and of the 5 different storm durations for both the wet and dry scenarios. The current Environment Canada data is also shown.

ECHAM5AOM_A1B	Return Period (years)					
	2	5	10	25	50	100
Duration (hours)						
1	52.38	71.31	85.89	107.01	124.90	144.78
2	68.99	94.33	114.21	143.53	168.78	197.24
6	88.20	120.55	146.33	184.88	218.53	256.91
12	103.39	136.43	162.22	200.06	232.50	268.91
24	118.43	154.48	181.86	221.06	253.88	289.98

Table 3.5(a): Depth of precipitation (mm) for ECHAM5AOM_A1B

MIROC3MEDRES_A2	Return Period (years)					
Duration (hours)	2	5	10	25	50	100
1	30.15	41.27	49.79	62.11	72.50	84.02
2	37.51	48.08	55.35	64.86	72.16	79.62
6	49.88	63.48	72.75	84.78	93.93	103.23
12	62.73	78.69	89.40	103.10	113.40	123.72
24	72.21	89.30	100.69	115.17	125.98	136.76

Table 3.5(b): Depth of precipitation (mm) for MIROC3MEDRES_A2

EC (1943-2003)	Return Period (years)					
Duration (hours)	2	5	10	25	50	100
1	24.40	35.30	42.50	51.60	58.30	65.00
2	29.60	41.60	49.50	59.60	67.00	74.40
6	36.60	48.20	55.80	65.40	72.50	79.60
12	43.00	54.70	62.50	72.40	79.70	87.00
24	51.30	66.80	77.10	90.00	99.60	109.20

Table 3.5(c): Depth of precipitation (mm) for Environment Canada

Table 3.6, shows the percent differences between the Environment Canada data, compared with both the wet and dry scenarios from the GEV distribution. There are drastic differences between the ECHAM5AOM_A1B (wet) scenario and the current EC values. On average, the wet scenario values are 84.46% higher than the EC values, with the greatest differences occurring for the 100-year return period in which 2 values are more than double the current EC standards.

The differences between the dry scenario and the EC values are not quite as severe, however the dry scenario average is still 24.16% larger than EC. In this case, the 2-hour return period has the largest differences occurring within it.

ECHAM5AOM_A1B	Return Period (years)					
Duration (hours)	2	5	10	25	50	100
1	72.88	67.56	67.59	69.87	72.71	76.06
2	79.91	77.59	79.06	82.64	86.34	90.44
6	82.70	85.75	89.57	95.48	100.35	105.38
12	82.51	85.53	88.75	93.71	97.89	102.22
24	79.10	79.25	80.91	84.27	87.29	90.58

Table 3.6(a): Percent Difference between ECHAM5AOM_A1B and EC

MIROC3MEDRES_A2	Return Period (years)					
Duration (hours)	2	5	10	25	50	100
1	21.08	15.58	15.80	18.48	21.72	25.53
2	23.57	14.44	11.15	8.46	7.42	6.78
6	30.71	27.36	26.37	25.80	25.76	25.85
12	37.32	35.97	35.42	34.99	34.90	34.85
24	33.86	28.83	26.54	24.54	23.39	22.41

Table 3.6(b): Percent Difference between MIROC3MEDRES_A2 and EC

The 2 scenarios shown represent the maximum and minimum outcomes of all the emission scenarios that were tested. By looking at these 2 extremes, we bypass the need to consider all of the uncertainties that are present when using the AOGCMs as all other scenario data will fit between the bounds of 2 extremes. However, due to the uncertainties in the models, these data sets do not provide an accurate estimate of the future extreme events, rather they display that the future precipitation events will not be similar to the historical data.

Table 3.7 shows the percent differences of the wet and dry scenarios, compared with the historical perturbed data.

ECHAM5AOM_A1B	Return Period (years)					
Duration (hours)	2	5	10	25	50	100
1	44.93	51.56	57.24	65.22	71.49	77.86
2	43.76	49.19	54.07	61.10	66.73	72.54
6	51.06	57.11	61.18	66.37	70.25	74.12
12	50.12	56.17	60.87	67.31	72.33	77.45
24	48.84	53.16	56.44	60.92	64.42	67.99

Table 3.7(a): Percent Difference between ECHAM5AOM_A1B and Historical Perturbed

MIROC3MEDRES_A2	Return Period (years)					
Duration (hours)	2	5	10	25	50	100
1	-9.51	-1.96	4.36	13.27	20.33	27.61
2	-16.43	-17.14	-16.96	-16.28	-15.55	-14.69
6	-4.79	-5.40	-6.69	-8.98	-11.05	-13.34
12	1.25	2.69	3.27	3.74	3.96	4.08
24	0.37	-0.33	-1.10	-2.28	-3.28	-4.35

Table 3.7(b): Percent Difference between MIROC3MEDRES_A2 and Historical Perturbed

The wet scenario shows a large increase of 61.06%, however the dry scenario shows a slight decrease of 2.84%. The EV1 statistics show the same wet scenario increasing at approximately 80%, while the dry scenario shows similar results. This shows that the EV1 distribution estimates higher values than GEV in the case of the UTRCA data.

(Solaiman, 2011)

3.4.1 Return Values

This report analyzed data from 27 different AOGCMs, each for durations of 1, 2, 6, 12 and 24-hour storms. Results shown are based strictly on GEV calculations.

The following figures show the return values for all scenarios of each storm duration.

Figures 3.3(a-e) show the relationship between the return period and the depth of precipitation for each AOGCM, at all 5 storm durations. For the 1-hour duration, the

minimum value is 60mm, and the maximum is 140mm at the 100-year return period. The minimum and maximum values for the 24-hour storm duration are 140mm and 290mm respectively. These figures show how with the application of the AOGCMs, the return values widely vary due to the assumptions made in each model.

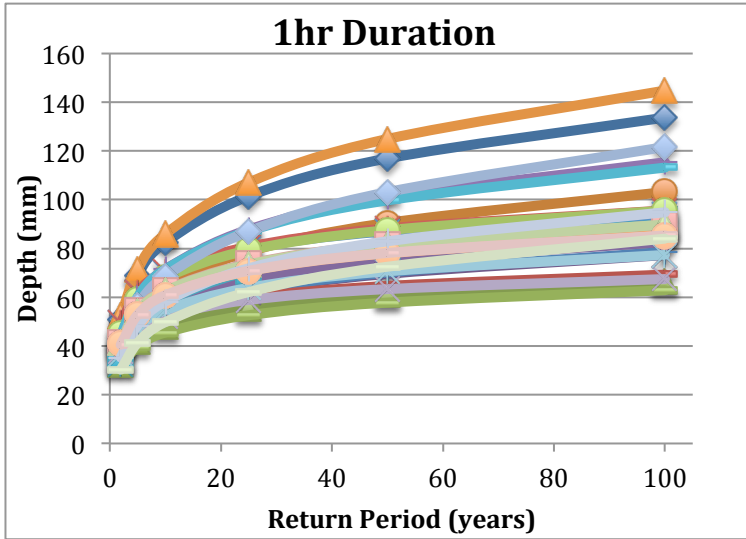


Figure 3.3(a): 1-Hour Duration Return Values

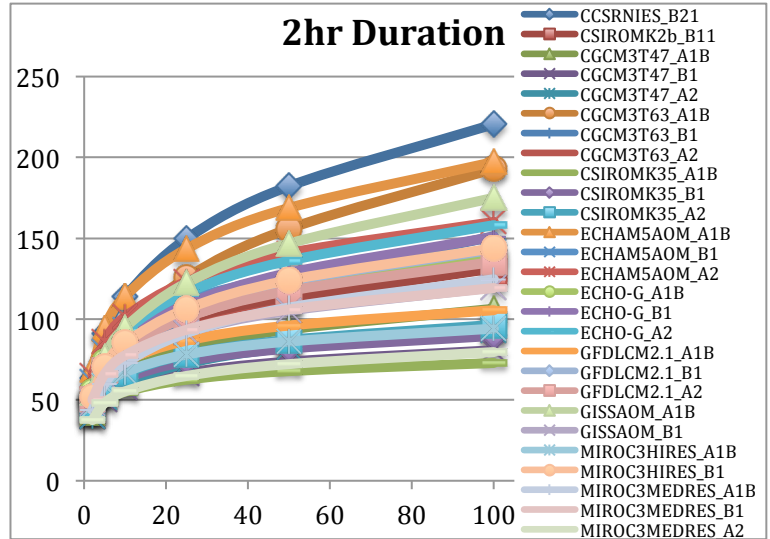


Figure 3.3(b): 2-Hour Duration Return Values

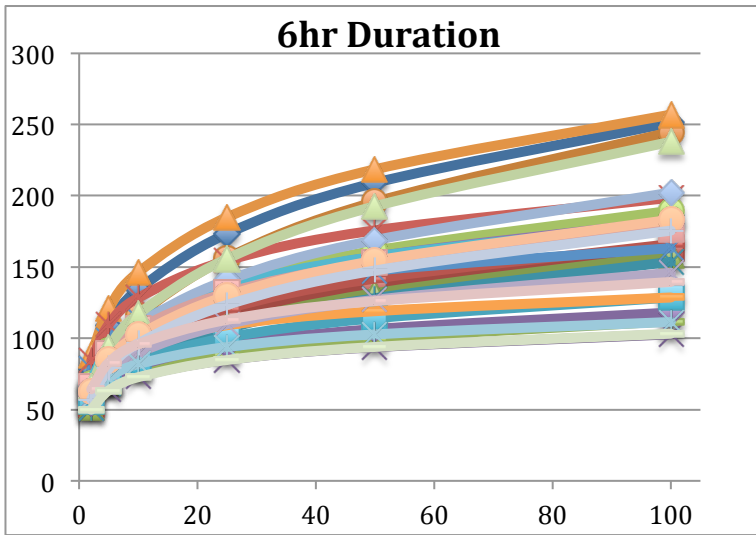


Figure 3.3(c): 6-Hour Duration Return Values

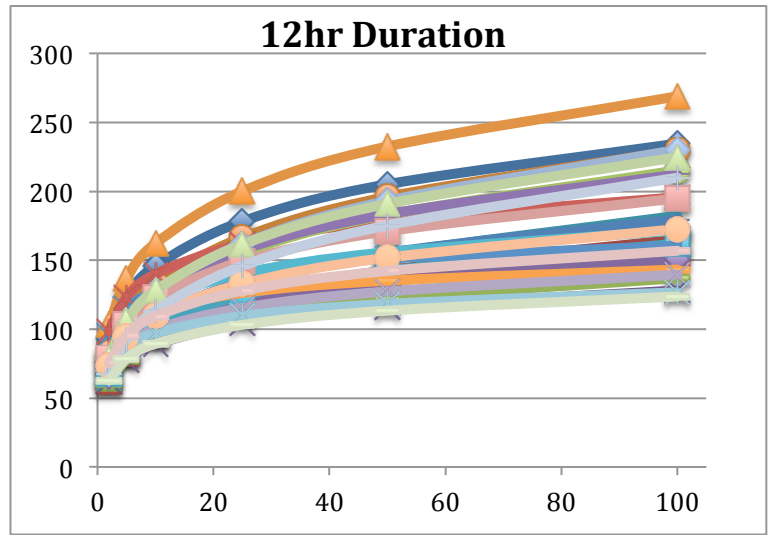


Figure 3.3(d): 12-Hour Duration Return Values

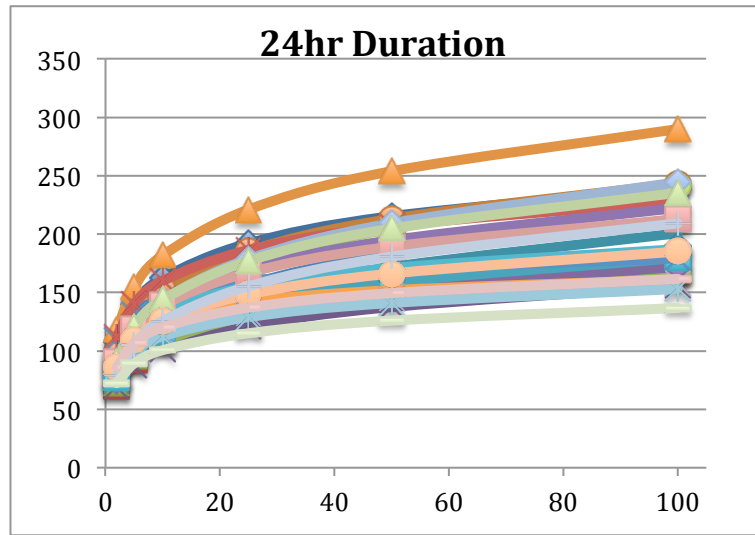


Figure 3.3(e): 24-Hour Duration Return Values

3.4.2 IDF Curves

The following figures show the 2, 5, 10, 25, 50 and 100 year return period IDF curves. These figures show the intensity (mm/hour) of precipitation for the 5 storm durations. Displayed in the figures are the wet and dry scenarios, as well as the resultant of the wet and dry scenarios, plotted against the historical perturbed data. The wet and dry scenarios are used as they produce the most extreme values, meaning that all other AOGCM models would fit between the 2 curves. In all 6 graphs the historical perturbed curve is very similar to the dry scenario (MIROC3MEDRES_A2).

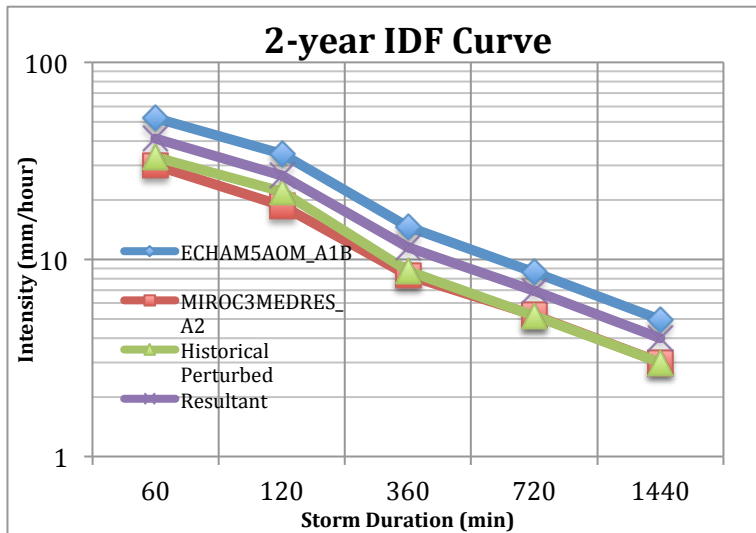


Figure 3.4(a): 2-Year IDF Curve

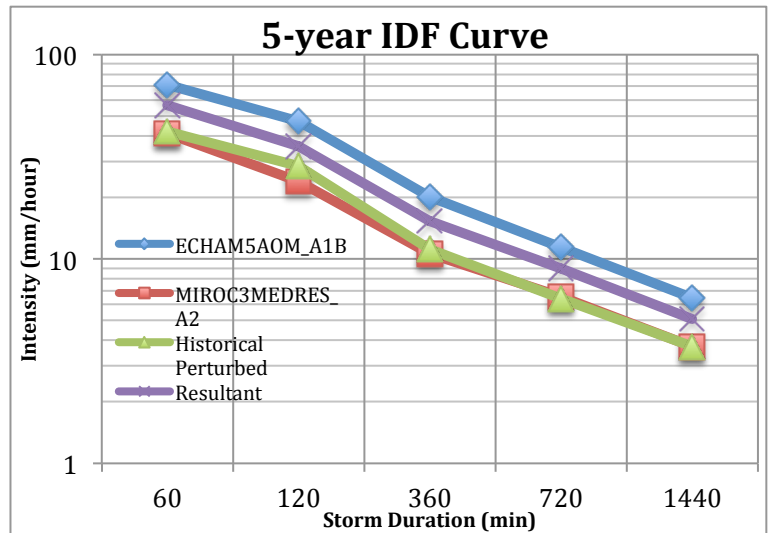


Figure 3.4(b): 5-Year IDF Curve

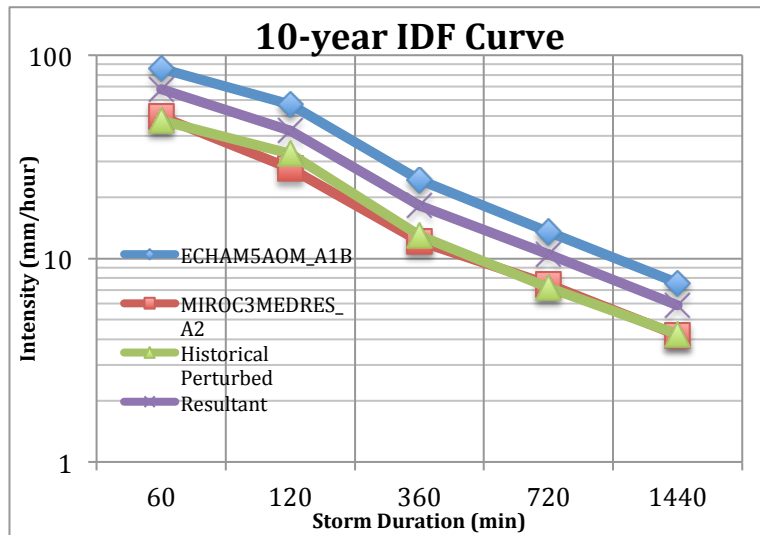


Figure 3.4(c):10-Year IDF Curve

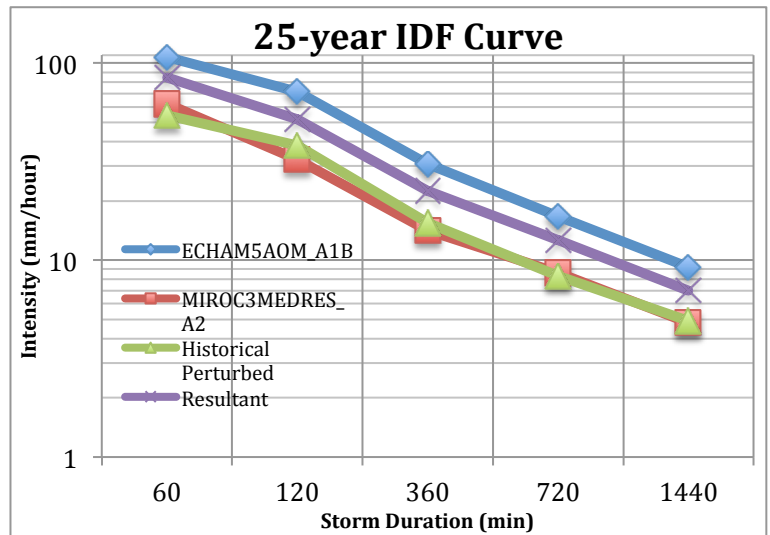


Figure 3.4(d):25-Year IDF Curve

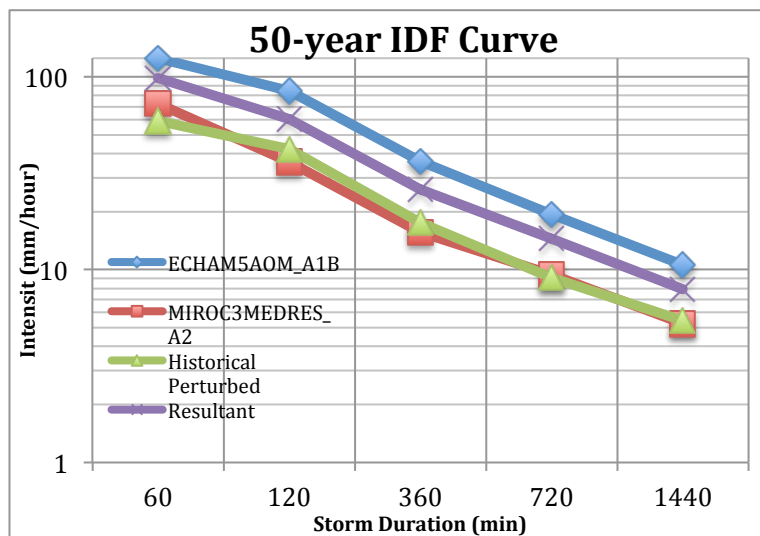


Figure 3.4(e):50-Year IDF Curve

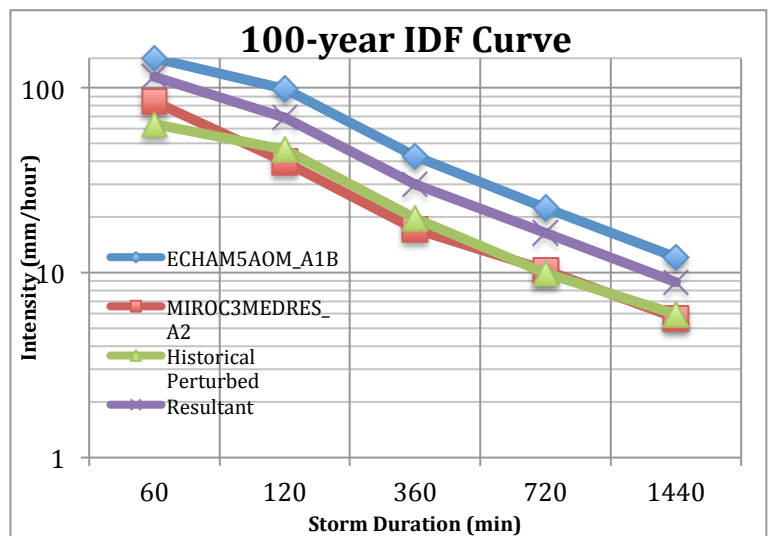


Figure 3.4(f):100-Year IDF Curve

4. Conclusions

Historical precipitation data and precipitation data sets derived from different AOGCMs for future climate for the London International Airport station has been used in this study to select an appropriate distribution for the estimation of design precipitation. 11 different AOGCMs were used to produce a total of 27 different synthetic data sets, each with 117 years of annual maximum precipitation data for storm durations of 1, 2, 6, 12 and 24 hours. The GEV distribution was compared with the Gumbel distribution, which is currently the standard in Canada, and the Log-Pearson type 3 distribution, which is the standard in the United States.

A variety of tests were used to determine if the synthetic data was an acceptable fit with the GEV distribution. The Anderson-Darling, Kolmogorov-Smirnov, and Chi-Squared tests were used to compare the goodness of fit between the 3 distributions. The GEV distribution was rejected the least number of times (14 times), at the 5% significance level, with EV1 being rejected the most (68 times). This shows that GEV cannot be excluded from one of the possible distributions, whereas EV1 showed a much weaker fit.

L-Moment Ratio diagrams were also used to help determine which distribution displayed the best fit for the data. In all 6 diagrams, the data seemed to follow the GEV distribution very well, much better than both LP3 and EV1.

The shape parameter of the GEV distribution was also analyzed, as a negative value is desired for practical applications as it ensures that the distribution is not upper-bounded. The average value was -0.108, with only 23 out of the 135 values being greater than 0. The 23 positive values were all very close to 0, further emphasizing the suitability of the GEV distribution for the Upper Thames watershed data.

The IDF curves are estimated in this report for historical data and data sets from different AOGCMs using the previously selected GEV distribution for London station.

As statistical models use many assumptions, the use of different AOGCMs ensures the uncertainties that are present in the calculation of IDF curves are included. A wide range of results was produced from these 27 different models, with a large difference between the minimum and maximum precipitation values. For the purpose of this study, no one model is being recommended. These results were produced to show how the GEV return values greatly vary from current Environment Canada standards, and that more research needs to be done to determine the validity of the results in this report. Some comparisons were made between the historical data and the current Environment Canada values. As 27 various models were used, the IDF curves show the 2 extreme models of the largest and smallest return values. Using the 2 extreme models ensures that we are taking into account all the uncertainties from the 27 models.

The GEV distribution has shown to be the strongest fitting distribution out of the 3 when using the data sets from the Upper Thames River Watershed. The need for more studies of the application of GEV distribution on other watersheds in Canada is recommended to ensure its countrywide applicability.

References

About the UTRCA. (2011). *Upper Thames River Conservation Authority*. Retrieved on July 26, 2011 from http://www.thamesriver.on.ca/About_Us/about.htm.

Cunnane, C. (1989). "Statistical Distributions For Flood Frequency Analysis". *Operational Hydrology Report* no. 33, World Meteorological Organization.

Das, S., (2010). "Estimation of Flood Estimation Techniques in the Irish Context". PhD thesis, Department of Engineering Hydrology, National University of Ireland Galway

Extremes- Gumbel. (2005). *Environment Canada*. Retrieved July 29, 2011 from <http://map.ns.ec.gc.ca/clchange/map/pages/GumbelIntro.aspx>.

Hosking, J.R.M., Wallis, J.R. (1997). "Regional Frequency Analysis". Cambridge University Press, Cambridge

http://climate.weatheroffice.ec.gc.ca/climateData/canada_e.html

IPPC, (2007). *Climate Change 2007: Working Group II: Impacts, Adaptation and Vulnerability*

Kochanek, K., Markiewicz, I., Strupczewski, W,G. (2010). "On Feasibility of L-Moments method for distributions with cumulative distribution function, and its inverse inexpressible in the explicit form". International Workshop: Advances in Statistical Hydrology. Taormina, Italy.

National Climate Data and Information Archive (2011). *Environment Canada*.

Nazemi, A. R. et al. (2011). "Uncertainties in the Estimation of Future Annual Extreme Daily Rainfall for the City of Saskatoon under Climate Change Effects". 20th Canadian Hydrotechnical Conference, CSCE

Prodanovic, P., Simonovic, S.P. (2006). "Inverse Flood Risk Modelling of The Upper Thames River Basin", *Water Resource Research Report* no. 052, Facility for Intelligent

Decision Support, Department of Civil and Environmental Engineering, The University of Western Ontario.

Rowinski, P. M., Strupczewski, W.G., Singh, V. P., (2001). "A note on the applicability of log-Gumbel and log-logistic probability distributions in hydrological analyses". *Hydrological Sciences Journal*

Solaiman, T.A., (2011). "Uncertainty Estimation of Extreme Precipitations Under Climatic Change: A Non-Parametric Approach". PhD Thesis, Department of Civil and Environmental Engineering, The University of Western Ontario

Stedinger, J.R., Griffis, V.W. (2007). "Log Pearson Type 3 Distribution and Its Application in Flood Frequency Analysis. I: Distribution Characteristics". *Journal of Hydrologic Engineering, ASCE*

Stedinger, J.R., Griffis, V.W. (2008). "Flood Frequency Analysis in the United States: Time to Update". *Journal of Hydrologic Engineering, ASCE*

Storch, H., Zwiers, F.W., (1999). "Statistical Analysis in Climate Change Research". Cambridge University Press, Cambridge

Vogel, R.M et al. (1993). "Flood-Flow Frequency Model Selection In Southwestern United States". *Journal of Water Resources Planning and Management*

Nakicenovic, N., Alcamo, J., Davis, G., de Vries, B., Fenhann, J., and co-authors. (2000). "IPCC Special Report on Emissions Scenarios". *UNEP/GRID-Arendal Publications*.

Appendix A: Figures

Figure A.1-A.6 show the L-moment ratio diagrams for the 5 durations used, and also include the historical unperturbed data set (A.6).

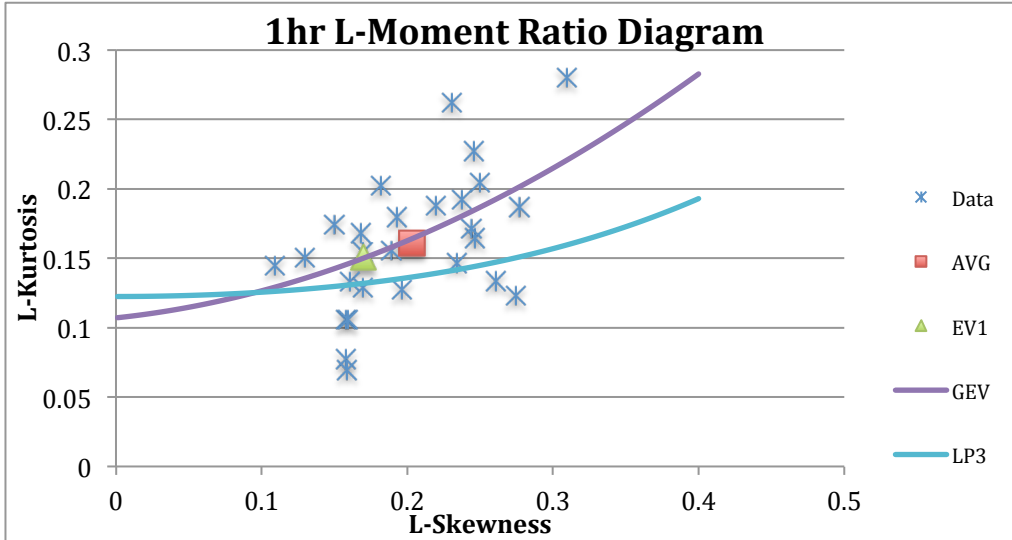


Figure A.1

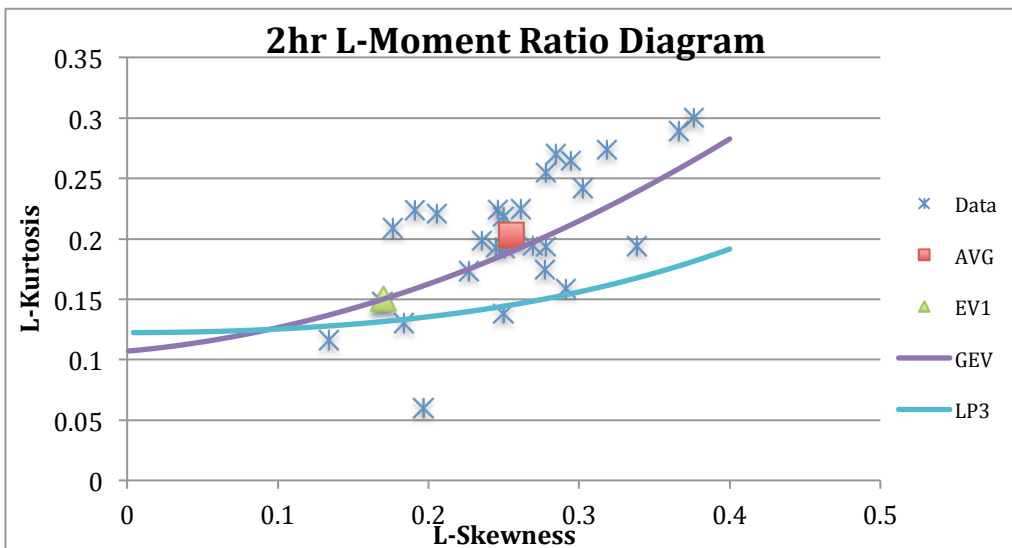


Figure A.2

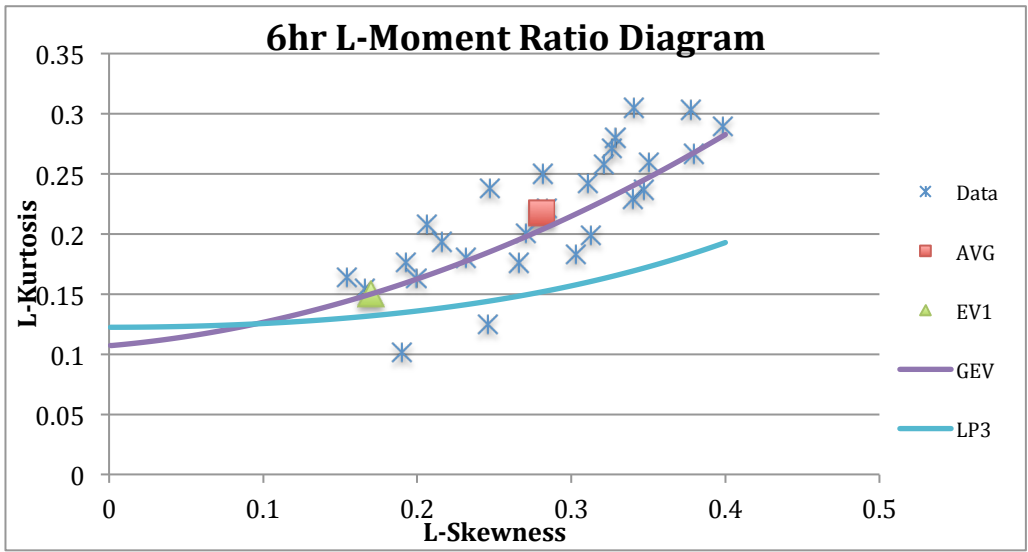


Figure A.3

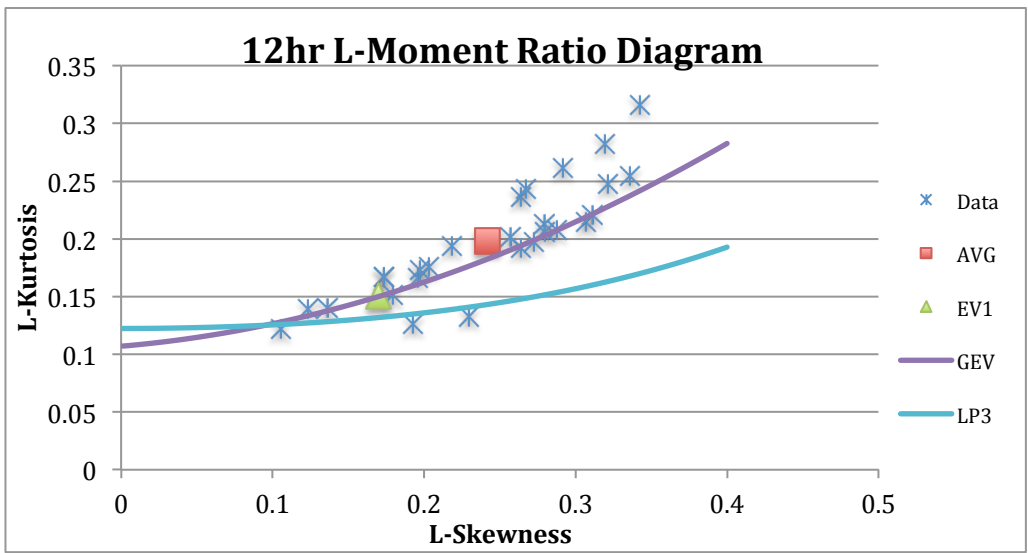


Figure A.4

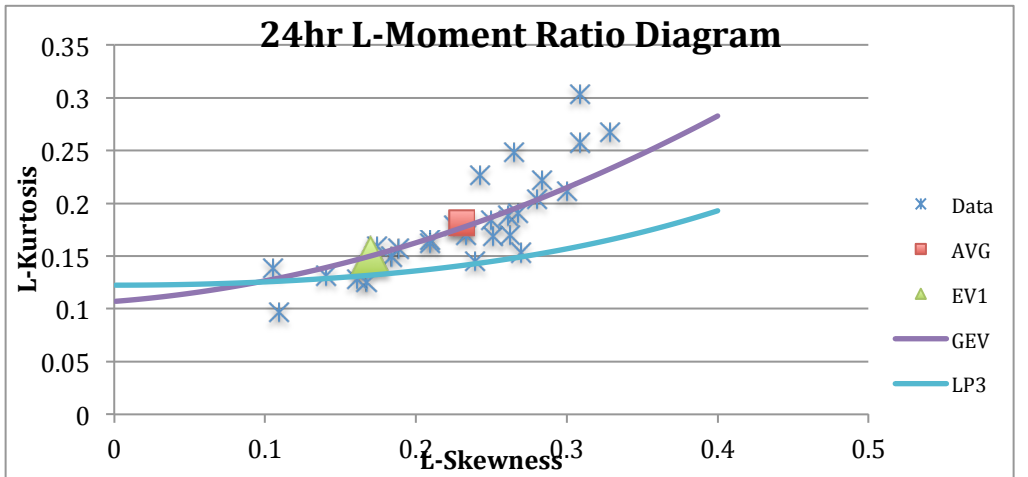


Figure A.5

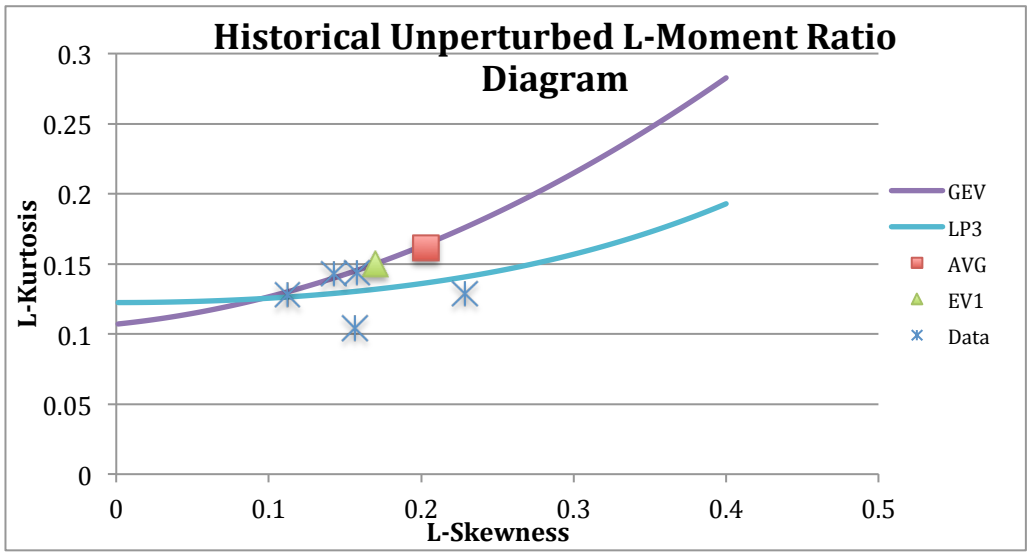


Figure A.6

Figure A.7-A.11 show the variation of shape parameter with respect to the AOGCMs for each of the 5 durations.

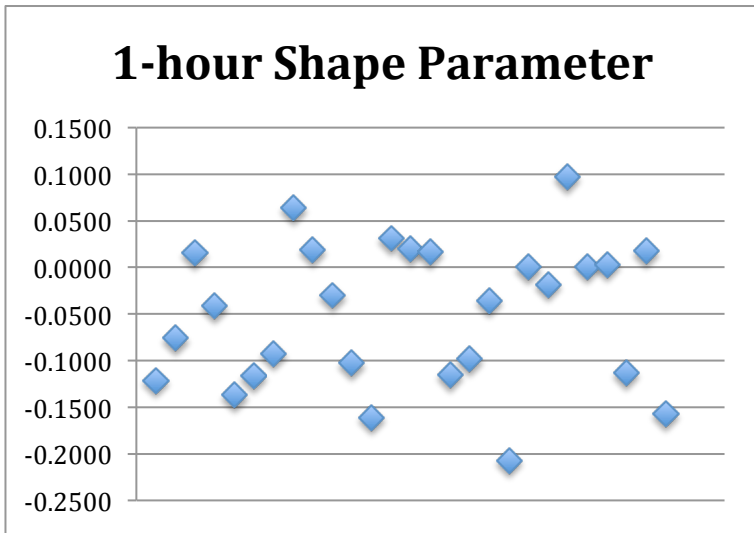


Figure A.7

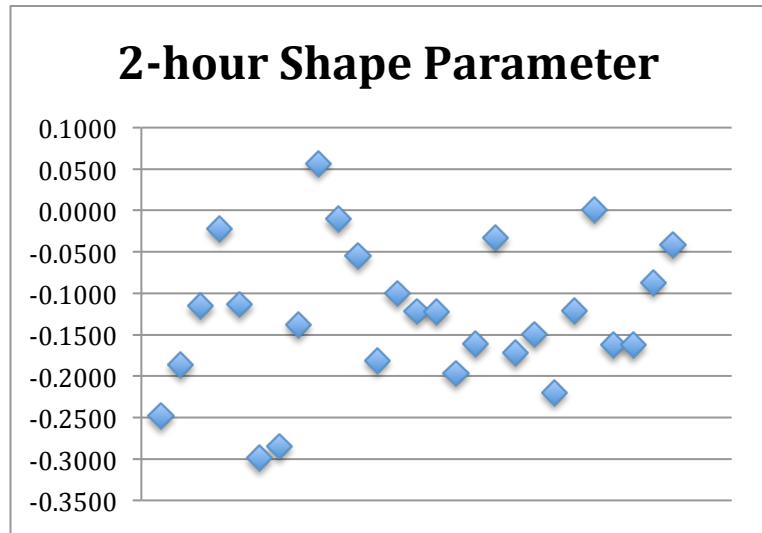


Figure A.8

6-hour Shape Parameter

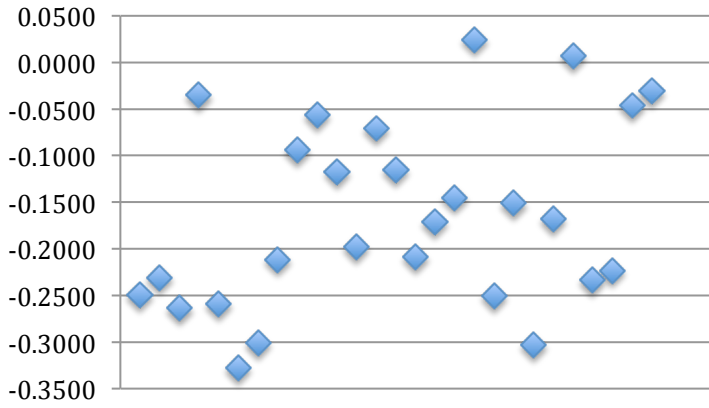


Figure A.9

12-hour Shape Parameter

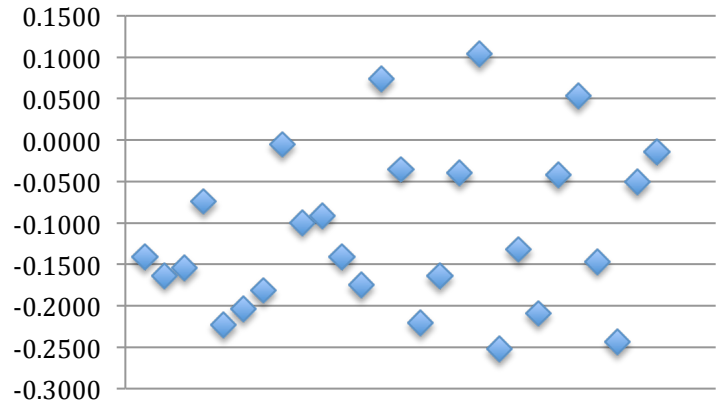


Figure A.10

24-hour Shape Parameter

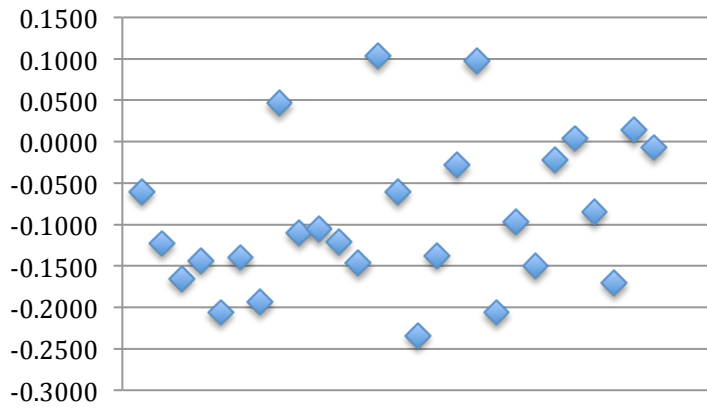


Figure A.11

Appendix B: Previous Reports in the Series

ISSN: (print) 1913-3200; (online) 1913-3219

(1) Slobodan P. Simonovic (2001). Assessment of the Impact of Climate Variability and Change on the Reliability, Resiliency and Vulnerability of Complex Flood Protection Systems. Water Resources Research Report no. 038, Facility for Intelligent Decision Support, Department of Civil and Environmental Engineering, London, Ontario, Canada, 91 pages. ISBN: (print) 978-0-7714- 2606-3; (online) 978-0-7714-2607-0.

(2) Predrag Prodanovic (2001). Fuzzy Set Ranking Methods and Multiple Expert Decision Making. Water Resources Research Report no. 039, Facility for Intelligent Decision Support, Department of Civil and Environmental Engineering, London, Ontario, Canada, 68 pages. ISBN: (print) 978-0-7714-2608-7; (online) 978-0-7714-2609-4.

(3) Nirupama and Slobodan P. Simonovic (2002). Role of Remote Sensing in Disaster Management. Water Resources Research Report no. 040, Facility for Intelligent Decision Support, Department of Civil and Environmental Engineering, London, Ontario, Canada, 107 pages. ISBN: (print) 978-0-7714-2610-0; (online) 978-0-7714- 2611-7.

(4) Taslima Akter and Slobodan P. Simonovic (2002). A General Overview of Multiobjective Multiple-Participant Decision Making for Flood Management. Water Resources Research Report no. 041, Facility for Intelligent Decision Support, Department of Civil and Environmental Engineering, London, Ontario, Canada, 65 pages. ISBN: (print) 978-0-7714-2612-4; (online) 978- 0-7714-2613-1.

(5) Nirupama and Slobodan P. Simonovic (2002). A Spatial Fuzzy Compromise Approach for Flood Disaster Management. Water Resources Research Report no. 042, Facility for Intelligent Decision Support, Department of Civil and Environmental Engineering, London, Ontario, Canada, 138 pages. ISBN: (print) 978-0-7714-2614-8; (online) 978-0-7714-2615-5.

(6) K. D. W. Nandalal and Slobodan P. Simonovic (2002). State-of-the-Art Report on Systems Analysis Methods for Resolution of Conflicts in Water Resources Management. Water Resources Research Report no. 043, Facility for Intelligent Decision Support, Department of Civil and Environmental Engineering, London, Ontario, Canada, 216 pages. ISBN: (print) 978-0-7714- 2616-2; (online) 978-0-7714-2617-9.

(7) K. D. W. Nandalal and Slobodan P. Simonovic (2003). Conflict Resolution Support System – A Software for the Resolution of Conflicts in Water Resource Management. Water Resources Research Report no. 044, Facility for Intelligent Decision Support, Department of Civil and Environmental Engineering, London, Ontario, Canada, 144 pages. ISBN: (print) 978-0-7714- 2618-6; (online) 978-0-7714-2619-3.

- (8) Ibrahim El-Baroudy and Slobodan P. Simonovic (2003). New Fuzzy Performance Indices for Reliability Analysis of Water Supply Systems. Water Resources Research Report no. 045, Facility for Intelligent Decision Support, Department of Civil and Environmental Engineering, London, Ontario, Canada, 90 pages. ISBN: (print) 978-0-7714-2620-9; (online) 978-0-7714- 2621-6.
- (9) Juraj Cunderlik (2003). Hydrologic Model Selection for the CFCAS Project: Assessment of Water Resources Risk and Vulnerability to Changing Climatic Conditions. Water Resources Research Report no. 046, Facility for Intelligent Decision Support, Department of Civil and Environmental Engineering, London, Ontario, Canada, 40 pages. ISBN: (print) 978-0-7714- 2622- 3; (online) 978-0-7714- 2623-0.
- (10) Juraj Cunderlik and Slobodan P. Simonovic (2004). Selection of Calibration and Verification Data for the HEC-HMS Hydrologic Model. Water Resources Research Report no. 047, Facility for Intelligent Decision Support, Department of Civil and Environmental Engineering, London, Ontario, Canada, 29 pages. ISBN: (print) 978-0-7714-2624-7; (online) 978-0-7714-2625-4.
- (11) Juraj Cunderlik and Slobodan P. Simonovic (2004). Calibration, Verification and Sensitivity Analysis of the HEC-HMS Hydrologic Model. Water Resources Research Report no. 048, Facility for Intelligent Decision Support, Department of Civil and Environmental Engineering, London, Ontario, Canada, 113 pages. ISBN: (print) 978- 0-7714-2626-1; (online) 978-0-7714- 2627-8.
- (12) Predrag Prodanovic and Slobodan P. Simonovic (2004). Generation of Synthetic Design Storms for the Upper Thames River basin. Water Resources Research Report no. 049, Facility for Intelligent Decision Support, Department of Civil and Environmental Engineering, London, Ontario, Canada, 20 pages. ISBN: (print) 978- 0-7714-2628-5; (online) 978-0-7714-2629-2.
- (13) Ibrahim El-Baroudy and Slobodan P. Simonovic (2005). Application of the Fuzzy Performance Indices to the City of London Water Supply System. Water Resources Research Report no. 050, Facility for Intelligent Decision Support, Department of Civil and Environmental Engineering, London, Ontario, Canada, 137 pages. ISBN: (print) 978-0-7714-2630-8; (online) 978-0-7714-2631-5.
- (14) Ibrahim El-Baroudy and Slobodan P. Simonovic (2006). A Decision Support System for Integrated Risk Management. Water Resources Research Report no. 051, Facility for Intelligent Decision Support, Department of Civil and Environmental Engineering, London, Ontario, Canada, 146 pages. ISBN: (print) 978-0-7714-2632-2; (online) 978-0-7714-2633-9.
- (15) Predrag Prodanovic and Slobodan P. Simonovic (2006). Inverse Flood Risk Modelling of The Upper Thames River Basin. Water Resources Research Report no. 052, Facility for Intelligent Decision Support, Department of Civil and Environmental Engineering, London, Ontario, Canada, 163 pages. ISBN: (print) 978-0-7714-2634-6;

(online) 978-0-7714-2635-3.

(16) Predrag Prodanovic and Slobodan P. Simonovic (2006). Inverse Drought Risk Modelling of The Upper Thames River Basin. Water Resources Research Report no. 053, Facility for Intelligent Decision Support, Department of Civil and Environmental Engineering, London, Ontario, Canada, 252 pages. ISBN: (print) 978-0-7714-2636-0; (online) 978-0-7714-2637-7.

(17) Predrag Prodanovic and Slobodan P. Simonovic (2007). Dynamic Feedback Coupling of Continuous Hydrologic and Socio-Economic Model Components of the Upper Thames River Basin. Water Resources Research Report no. 054, Facility for Intelligent Decision Support, Department of Civil and Environmental Engineering, London, Ontario, Canada, 437 pages. ISBN: (print) 978-0-7714-2638-4; (online) 978-0-7714-2639-1.

(18) Subhankar Karmakar and Slobodan P. Simonovic (2007). Flood Frequency Analysis Using Copula with Mixed Marginal Distributions. Water Resources Research Report no. 055, Facility for Intelligent Decision Support, Department of Civil and Environmental Engineering, London, Ontario, Canada, 144 pages. ISBN: (print) 978-0-7714-2658-2; (online) 978-0-7714-2659-9.

(19) Jordan Black, Subhankar Karmakar and Slobodan P. Simonovic (2007). A Web-Based Flood Information System. Water Resources Research Report no. 056, Facility for Intelligent Decision Support, Department of Civil and Environmental Engineering, London, Ontario, Canada, 133 pages. ISBN: (print) 978-0-7714-2660-5; (online) 978-0-7714-2661-2.

(20) Angela Peck, Subhankar Karmakar and Slobodan P. Simonovic (2007). Physical, Economical, Infrastructural and Social Flood Risk – Vulnerability Analyses in GIS. Water Resources Research Report no. 057, Facility for Intelligent Decision Support, Department of Civil and Environmental Engineering, London, Ontario, Canada, 80 pages. ISBN: (print) 978-0-7714-2662-9; (online) 978-0-7714-2663-6.

(21) Predrag Prodanovic and Slobodan P. Simonovic (2007). Development of Rainfall Intensity Duration Frequency Curves for the City of London Under the Changing Climate. Water Resources Research Report no. 058, Facility for Intelligent Decision Support, Department of Civil and Environmental Engineering, London, Ontario, Canada, 51 pages. ISBN: (print) 978-0-7714-2667-4; (online) 978-0-7714-2668-1.

(22) Evan G. R. Davies and Slobodan P. Simonovic (2008). An integrated system dynamics model for analyzing behaviour of the social-economic-climatic system: Model description and model use guide. Water Resources Research Report no. 059, Facility for Intelligent Decision Support, Department of Civil and Environmental Engineering, London, Ontario, Canada, 233 pages. ISBN: (print) 978-0-7714-2679-7; (online) 978-0-

7714-2680-3.

(23) Vasana Arunachalam (2008). Optimization Using Differential Evolution. Water Resources Research Report no. 060, Facility for Intelligent Decision Support, Department of Civil and Environmental Engineering, London, Ontario, Canada, 42 pages. ISBN: (print) 978-0-7714- 2689- 6; (online) 978-0-7714-2690-2.

(24) Rajesh Shrestha and Slobodan P. Simonovic (2009). A Fuzzy Set Theory Based Methodology for Analysis of Uncertainties in Stage-Discharge Measurements and Rating Curve. Water Resources Research Report no. 061, Facility for Intelligent Decision Support, Department of Civil and Environmental Engineering, London, Ontario, Canada, 104 pages. ISBN: (print) 978-0-7714- 2707-7; (online) 978-0-7714-2708-4.

(25) Hyung-II Eum, Vasana Arunachalam and Slobodan P. Simonovic (2009). Integrated Reservoir Management System for Adaptation to Climate Change Impacts in the Upper Thames River Basin. Water Resources Research Report no. 062, Facility for Intelligent Decision Support, Department of Civil and Environmental Engineering, London, Ontario, Canada, 81 pages. ISBN: (print) 978-0-7714-2710-7; (online) 978-0-7714-2711-4.

(26) Evan G. R. Davies and Slobodan P. Simonovic (2009). Energy Sector for the Integrated System Dynamics Model for Analyzing Behaviour of the Social- Economic- Climatic Model. Water Resources Research Report no. 063. Facility for Intelligent Decision Support, Department of Civil and Environmental Engineering, London, Ontario, Canada. 191 pages. ISBN: (print) 978-0-7714- 2712-1; (online) 978-0-7714-2713-8.

(27) Leanna King, Tarana Solaiman, and Slobodan P. Simonovic (2009). Assessment of Climatic Vulnerability in the Upper Thames River Basin. Water Resources Research Report no. 064, Facility for Intelligent Decision Support, Department of Civil and Environmental Engineering, London, Ontario, Canada, 61pages. ISBN: (print) 978-0-7714-2816-6; (online) 978-0-7714- 2817- 3.

(28) Slobodan P. Simonovic and Angela Peck (2009). Updated Rainfall Intensity Duration Frequency Curves for the City of London under Changing Climate. Water Resources Research Report no. 065, Facility for Intelligent Decision Support, Department of Civil and Environmental Engineering, London, Ontario, Canada, 64pages. ISBN: (print) 978-0-7714-2819-7; (online) 987- 0-7714-2820-3.

(29) Leanna King, Tarana Solaiman, and Slobodan P. Simonovic (2010). Assessment of Climatic Vulnerability in the Upper Thames River Basin: Part 2. Water Resources Research Report no. 066, Facility for Intelligent Decision Support, Department of Civil and Environmental Engineering, London, Ontario, Canada, 72pages. ISBN: (print) 978-0-7714-2834-0; (online) 978- 0-7714-2835-7.

(30) Christopher J. Popovich, Slobodan P. Simonovic and Gordon A. McBean (2010). Use of an Integrated System Dynamics Model for Analyzing Behaviour of the Social-Economic-Climatic System in Policy Development. Water Resources Research

Report no. 067, Facility for Intelligent Decision Support, Department of Civil and Environmental Engineering, London, Ontario, Canada, 37 pages. ISBN: (print) 978-0-7714-2838-8; (online) 978-0-7714-2839-5.

(31) Hyung-II Eum and Slobodan P. Simonovic (2009). City of London: Vulnerability of Infrastructure to Climate Change; Background Report 1 – Climate and Hydrologic Modeling. Water Resources Research Report no. 068, Facility for Intelligent Decision Support, Department of Civil and Environmental Engineering, London, Ontario, Canada, 102pages. ISBN: (print) 978-0- 7714-2844-9; (online) 978-0-7714-2845-6.

(32) Dragan Sredojevic and Slobodan P. Simonovic (2009). City of London: Vulnerability of Infrastructure to Climate Change; Background Report 2 – Hydraulic Modeling and Floodplain Mapping. Water Resources Research Report no. 069, Facility for Intelligent Decision Support, Department of Civil and Environmental Engineering, London, Ontario, Canada, 147 pages. ISBN: (print) 978-0-7714-2846-3; (online) 978-0-7714-2847-0.

Processing:

(33) Tarana A. Solaiman and Slobodan P. Simonovic (January 2011). Assessment of Global and Regional Reanalyses Data for Hydro-Climatic Impact Studies in the Upper Thames River Basin. Water Resources Research Report no. 070, Facility for Intelligent Decision Support, Department of Civil and Environmental Engineering, London, Ontario, Canada, XXX pages. ISBN: (print) XXX- X-XXXX-XXXX-X; (online) XXX-X-XXXX-XXXX-X.

(34) Tarana A. Solaiman and Slobodan P. Simonovic (February 2011). Quantifying Uncertainties in the Modelled Estimates of Extreme Precipitation Events at the Upper Thames River Basin. Water Resources Research Report no. 071, Facility for Intelligent Decision Support, Department of Civil and Environmental Engineering, London, Ontario, Canada, XXX pages. ISBN: (print) XXX- X-XXXX-XXXX-X; (online) XXX-X-XXXX-XXXX-X.

(35) Tarana A. Solaiman and Slobodan P. Simonovic (March 2011). Development of Probability Based Intensity-Duration-Frequency Curves under Climate Change. Water Resources Research Report no. 072, Facility for Intelligent Decision Support, Department of Civil and Environmental Engineering, London, Ontario, Canada, XXX pages. ISBN: (print) XXX-X-XXXX-XXXX-X; (online) XXX-X-XXXX-XXXX-X.

(36) Dejan Vucetic and Slobodan P. Simonovic (April 2011). Water Resources Decision Making Under Uncertainty. Water Resources Research Report no. 073, Facility for Intelligent Decision Support, Department of Civil and Environmental Engineering, London, Ontario, Canada, XXX pages. ISBN: (print) XXX-X-XXXX-XXXX-X; (online) XXX-X-XXXX-XXXX-X.

(37) Angela Peck, Elisabeth Bowering and Slobodan P. Simonovic (November 2010). City of London: Vulnerability of Infrastructure to Climate Change, Final Report - Risk

Assessment. Water Resources Research Report no. 074, Facility for Intelligent Decision Support, Department of Civil and Environmental Engineering, London, Ontario, Canada, XXX pages. ISBN: (print) XXX- X-XXXX-XXXX-X; (online) XXX-X-XXXX-XXXX-X.

(38) Akhtar, M. K., S. P. Simonovic, J. Wibe, J. MacGee, and J. Davies, (2011). An integrated system dynamics model for analyzing behaviour of the social-energy-economy-climate system: model description. Water Resources Research Report no. 075, Facility for Intelligent Decision Support, Department of Civil and Environmental Engineering, London, Ontario, Canada, 210 pages. ISBN: (print) XXX-X-XXXX-XXXX-X; (online) XXX-X-XXXX-XXXX-X.

(39) Akhtar, M. K., S. P. Simonovic, J. Wibe, J. MacGee, and J. Davies, (2011). An integrated system dynamics model for analyzing behaviour of the social-energy-economy-climate system: user's manual. Water Resources Research Report no. 076, Facility for Intelligent Decision Support, Department of Civil and Environmental Engineering, London, Ontario, Canada, 161 pages. ISBN: (print) XXX-X-XXXX-XXXX-X; (online) XXX-X-XXXX-XXXX-X.